https://doi.org/10.5194/egusphere-2023-895
Preprint. Discussion started: 20 June 2023

Measurement Report: Optical Characterization, Seasonality, and Sources of Brown Carbon in Fine Aerosols from Tianjin, North China: Year-round Observations

Zhichao Dong[1], Chandra Mouli Pavuluri[1]*, Peisen Li[1], Zhanjie Xu[1], Junjun Deng[1], Xueyan Zhao[1], Xiaomai Zhao[1], Pingqing Fu[1], Cong-Qiang Liu[1]

[1]Institute of Surface-Earth System Science, School of Earth System Science, Tianjin University, Tianjin 300072, China

Correspondence to: Chandra Mouli Pavuluri (cmpavuluri@tju.edu.cn)

Abstract

To investigate the physicochemical characteristics and sources of brown carbon (BrC) in North China, we collected fine aerosols ($PM_{2.5}$) at an urban site in Tianjin over a 1-year period. We measured the ultraviolet (UV) light absorption and excitation emission matrix (EEM) fluorescence of the water-soluble BrC (WSBrC) and the water-insoluble but methanol-soluble BrC (WI-MSBrC) in the $PM_{2.5}$ using a three-dimensional fluorescence spectrometer. Average light absorption efficiency of both WSBrC ($Abs_{365,\ WSBrC}$) and WI-MSBrC ($Abs_{365,\ WI\text{-}MSBrC}$) at 365 nm was found to be highest in winter and distinct from season to season. Averages of biological index (BIX) and fluorescence index (FI) of WSBrC were lower in summer than in other seasons and opposite to that of humification index (HIX), which implied that the secondary formation and further chemical processing of aerosols were intensive during the summer period than in other seasons. Whereas in winter, the higher HIX together with the higher BIX and FI of WI-MSBrC suggested that the BrC loading was mainly influenced by primary emissions and was relatively water-soluble. Based on EEM, the types of chromophores in BrC were divided into humic-like substances (HULIS), including low-oxygenated and high-oxygenated species, and protein like compounds (PLOM). The direct radiation absorption caused by WSBrC and WI-MSBrC combinedly in the range of 300–400 nm was accounted for about 40% to the total radiation (range, 300–700 nm), which emphasizes that the radiation balance of the Earth's climate system is substantially affects by the BrC and should be considered in the radiative forcing models.

1 Introduction

Brown carbon (BrC) is a part of organic aerosol (OA) and has the ability to absorb solar radiation in the near-ultraviolet (UV) to visible spectrum (Liu et al., 2013). In the range of near-UV/Vis light (300–500 nm), BrC has a significant effect on radiative forcing in both regional and global climate (Feng et al., 2013; Jo et al., 2016; Park et al., 2010). However, the warming effect of water-soluble BrC in the Arctic has been reported to be accounted for about 30% of that of the black carbon (Yue et al., 2022). BrC not only affects the direct radiative forcing by OA, but also has a potential impact on indirect radiative forcing due to its hydrophilicity, which influences the formation of cloud condensation nuclei (CCN) (Andreae and Gelencs´er, 2006; Laskin et al., 2015). In addition, BrC is mostly composed of highly conjugated aromatic ring compounds (such as a polycyclic aromatic hydrocarbons) and high molecular weight substances with a polar functional

https://doi.org/10.5194/egusphere-2023-895
Preprint. Discussion started: 20 June 2023

group such as oxygen or nitrogen, or a humic-like substances (HULIS), which can cause a risk to human health. *For example*, carbon-containing aromatic compounds can cause physical weakness, decreased immunity, arteriosclerosis, etc., which will increase the mortality due to cardiovascular and cerebrovascular diseases and a variety of cancers such as skin cancer, pharyngeal cancer and nasal cancer (Diggs et al., 2011; Peters et al., 2008; Hecobian et al., 2010).

BrC can be emitted directly from primary sources and produced by chemical reactions of volatile organic compounds (VOCs) in the atmosphere (Chakrabarty et al., 2010; Jacobson, 1999; Sareen et al., 2010). Primary sources of BrC are combustion processes such as biomass burning (Hoffer et al., 2006; Brown et al., 2021), fossil fuel combustion (Jo et al., 2016), automobile exhaust (Liu et al., 2015) and non-combustion processes such as bioaerosols (plant debris and fungi) and soil humus (Lin et al., 2014; Rizzo et al., 2013; Rizzo et al., 2011). On the other hand, secondary BrC can be produced from complex chemical reactions of VOCs emitted from both anthropogenic and biological origin (Kasthuriarachchi et al., 2020; Li et al., 2020a).

After establishing the fact that organic compounds also absorb the light in recent times, the researchers are paying significant attention to the estimations of physical (optical) and chemical properties the BrC. Excitation emission matrix (EEM) fluorescence spectroscopy and ultraviolet spectroscopy are common techniques for studying the optical absorption and fluorescence chromophore optical and structural characteristics of complex organic materials (Chen et al., 2016b). Combined spectrophotometric measurement and chemical analysis has been applied to study the BrC in Xi 'an, Northwest China from July 2008 to June 2009 (Huang et al., 2018). Recently, the absorption spectroscopy of BrC has been used as a tool for understanding broader composition and characteristics of the BrC (Satish and Rastogi, 2019).

EEM provides some information about the chromophores responsible for the light absorption of organic matter. The fluorescence technique has been widely applied to measure organics in terrestrial and oceanic systems (Murphy et al., 2013; Yu et al., 2015), but has not been widely used in the study of atmospheric aerosols. The composition of humic-like and protein-like components have been identified from the analysis of chromophores of dissolved organic substances in aquatic environments (Xie et al., 2020). Fluorescence measurements with higher detection sensitivity are more useful in classifying BrC compared to absorption measurements, which rely on the shape of absorption spectra (Laskin et al., 2015). In recent times, the application of fluorescence technology has been well established to study the chemical composition of atmospheric aerosols (Wu et al., 2021; Deng et al., 2022; Li et al., 2022; Cao et al., 2022).

However, the studies on BrC are very limited because of difficulties in quantitative measurement of organic components and the optical properties of the BrC (Corbin et al., 2019; Wang et al., 2022b). In addition, traditional optical instruments do not provide any distinction between the light absorption by black and brown carbon. Therefore, the indirect approach to explore the nature and sources of BrC has been developed through its light absorption characteristics. Of course, such research is just at preliminary stages, and much attention need to be paid further such as long-term and continuous observations of light absorption characteristics of water-soluble BrC (WSBrC) and their temporal and spatial variations (Izhar et al., 2020). Moreover, the investigation of light absorption characteristics of water-insoluble BrC (WIBrC) that can be extracted into a solvent with higher extraction efficiency is necessary to better understand the impact of the BrC on climate change (Corbin et al., 2019). In fact, such studies are very scarce because the selection of solvents and determination of extraction efficiency are difficult, although different polar chromophores could be extracted by solvent extraction according to the polarity of solvent and methanol has been used as a common solvent (Chen et al., 2016a).

https://doi.org/10.5194/egusphere-2023-895
Preprint. Discussion started: 20 June 2023

Therefore, the comprehensive study of the optical properties of WSBrC and WIBrC is highly necessary to better understand the types of chromophores and optical properties of atmospheric aerosols, as well as the processes of oxidation and transformation of chromophores at different locale over the world.

China is one of the most polluted areas in the world, and suffering from the absorption and scattering of solar radiation by atmospheric aerosols that directly affect the energy balance of the Earth's climate system, especially in North China Plain (Wang et al., 2022a). As an important port city in the North China Plain, Tianjin, which has a large population, has received a widespread attention to address the atmospheric environmental issues. Previous studies have shown that BrC in the atmosphere contributes significantly to the light absorption by aerosols (Deng et al., 2022). $PM_{2.5}$ in the Tianjin area are extremely high and contain a lot of organic matter (OM) (Dong et al., 2023). In such an environment, BrC is likely to become an important light-absorbing component of atmospheric aerosols. However, the studies on physicochemical characteristics and sources of BrC are very limited in the North China Plain, and to the best of our knowledge, the long-term observations have not been reported yet over the Tianjin region.

In this study, we measured the optical properties of WSBrC and water-insoluble but methanol-soluble BrC (WI-MSBrC) in fine aerosols ($PM_{2.5}$) collected from Tianjin, North China over a one year period during 2018–2019. We discuss the seasonal variations in optical properties of WSBrC and WI-MSBrC and their chromophore composition assessed by three-dimensional fluorescence spectroscopy. We also assess the relationship between BrC and chemical composition in $PM_{2.5}$, the possible sources of BrC and the influence of photochemical reaction processes on the BrC. Thus, this study provides a comprehensive understanding of the optical characteristics, seasonality and sources of BrC in the Tianjin region, and the need to develop the prevention and control strategies for the BrC emissions.

2 Materials and Methods

2.1 Aerosol sampling

Fine aerosol ($PM_{2.5}$) sampling was conduted in Tianjin, a coastal city located at the lower reaches of the Haihe River and Bohai Sea and 150 km away from Beijing in the northern part of China. The sampling took place on the rooftop of a six-storey building at Tianjin University (ND, 39.11°N,117.18°E) in an urban area of Nankai District, Tianjin. A high-volume air sampler (Tisch Environmental, TE-6070DX) at a flow rate of 1.0 m^3 min^{-1} and pre-combusted (6 hours at 450°C) quartz fiber filters (Pallflex 2500QAT-UP) were used for continuously collecting the $PM_{2.5}$ samples for 3 days (~72 hours) each during 5 July 2018 to 4 July 2019 (n = 121). Filter blanks were collected twice per season during the sample period, using the same procedure as regular sampling, but without turning on the sampler pump. The blank filters were left in the filter hood for 10 minutes. Prior to and after sampling, each filter was dehumidified in a desiccator for 48 hours, and then stored in a pre-combusted glass jar with a Teflon-lined cap in the dark at −20°C until analysis.

2.2 Chemical analysis

Details of the measurements of aerosol OC, EC, total carbon (TC), and WSOC were described by Wang et al. (Wang et al., 2019) and Dong et al. (Dong et al., 2023). Briefly, concentrations of the OC and EC were measured with a thermal-optical transmission analyzer (Sunset Laboratory

https://doi.org/10.5194/egusphere-2023-895
Preprint. Discussion started: 20 June 2023

Inc, USA) following the IMPROVE protocol of the protective visual environment. Stable carbon and nitrogen isotope ratios of total carbon and nitrogen were measured with an elemental analyzer (EA, Flash 2000HT) coupled with stable isotope ratio mass spectrometer (IrMS, 253 Plus). Concentrations of K^+ and Cl^- were determined using ion chromatography (ICS-5000 System, China, Dai An).

BrC was extracted into 30 ml ultrapure water (>18.2MΩ cm) using a sample filter disc of 22 mm in diameter under ultrasonication for 30 min. The extracts were filtered through a 0.45 μm polytetrafluoron (PTFE) syringe filter to remove the water-insoluble compounds, and then transferred into another clean glass bottle. The extracts were used for the light absorption and fluorescence measurements of WSBrC. While the concentration of WSBrC was considered as the concentration of water-soluble organic carbon (WSOC).

After the extraction of WSBrC, the WI-MSBrC was extracted into 30 ml methanol using the same filter sample under ultrasonication for 30 min. The extracts were filtered using the same 0.45 μm PTFE syringe filter to remove the insoluble particles and filter debris. The methanol extracts were used for the measurements of optical properties of WI-MSBrC. The concentration of water-insoluble organic carbon (WIOC) was considered as the concentration of WI-MSBrC, which calculated as: WI-MSBrC = OC − WSOC.

2.3 Optical properties of brown carbon (BrC) analysis

2.3.1 Light absorption analysis

A three-dimensional fluorescence spectrometer (Aqualog, Horiba Scientific) was used to record the excitation-emission matrices (EEM) spectra and ultraviolet-visible (UV–Vis) absorption spectra of the solution samples in 1×1 cm quartz cuvettes. The instrument parameters during sample analysis were as follows: The UV-Vis absorption spectra of extracts were recorded in the wavelength range of 240–700 nm. The UV−visible absorption spectra of the solvents were also recorded to subtract their contributions from the extract spectra. The EEM was recorded in the wavelength range of 240–700 nm for excitation and the integration time was 0.1 s with a 1 nm increment. An increment of 8 pixels (5.04 nm) is used as the emission wavelength interval. Prior to sample analysis, a fluorescence spectrometer wae used to anlyze the pure solvents of water and MeOH to obtain the reference signal.

Based on the light absorption spectra, the absorption data are converted to the absorption coefficient (Abs: m^{-1}) following this formula:

$$Abs_\lambda = (A_\lambda - A_{700}) \times V_l / V_a / L \times \ln(10)$$

where A_{700} is the absorption at 700 nm, serving as a reference to account for baseline drift; V_l is the volume of water or MeOH used for extraction; V_a is the volume of sampled air; L is the optical path length (0.01 m). A factor of ln(10) is utilized to convert the log base 10 to a natural logarithm to obtain a base-e absorption coefficient. To compensate for any baseline shift that may occur during analysis, absorption at wavelengths below 700 nm is compared to that of 700 nm where no absorption occurs for ambient aerosol extracts. The average absorption coefficient between 360 and 370 nm (Abs_{365}) is used to represent BrC absorption in order to avoid any interferences from non-organic compounds (e.g., nitrate) and to be consistent with the literature values (Huang et al., 2018).

Absorption Ångström exponent (AAE, Å) represents the spectral dependence of aerosol light absorption, indicating that BrC has a great contribution to aerosol Absorption. The spectral

https://doi.org/10.5194/egusphere-2023-895
Preprint. Discussion started: 20 June 2023

dependence of light absorption by chromophores in solution can be described by the following equation:

$$Abs_\lambda = C \times \lambda^{-AAE}$$

where C is a concentration of extract; λ is the wavelength (nm). The AAE of the filter extracts is calculated by a formula in the wavelength range of 300–500 nm. The selected range serves two purposes: (1) to prevent any interferences from non-organic compounds at lower wavelengths; (2) to ensure a sufficiented signal-noise ratio for the investigating samples (Huang et al., 2018).

The mass absorption efficiency (MAE: $m^2\ g^{-1}$) of the filter extract at wavelength of λ can be characterized as:

$$MAE_\lambda = Abs_\lambda/M$$

where M (μg m^{-3}) is the concentration of WSOC for water extracts and that of WIOC for methanol extracts.

The imaginary part (*k*) of the refractive index (m = n+i*k*) is derived with the following equation:

$$k_\lambda = (MAC \times \rho \times \lambda)/4\pi$$

where MAC is the mass-absorption cross section of WSBrC or WI-MSBrC ($m^2\ g^{-1}$), ρ is the effective density, λ is the wavelength for the computed MAC including WSBrC and WI-MSBrC. For this study, an effective density of 1.5 g m^{-3} is assumed for WSBrC and WI-MSBrC in the derivation (Liu et al., 2013). MAC values are computed for 365 nm.

2.3.2 EEM and PARAFAC analysis

The raw EEMs were first calibrated for the correction of spectrometer factors, which reflect the spectrometer deviation and light source, and then for the inner filter correction, following the procedure described elsewhere (Chen et al., 2019; Gu and Kenny, 2009). Briefly, the inner filter correction of the EEMs was done based on the UV-Vis light absorbance of the extracts, which was lower than 0.7 in the calibrated wavelength range and is appropriate (Gu and Kenny, 2009). The signal intensity of the EEMs was then normalized to the Raman unit (RU) of water (Lawaetz and Stedmon, 2009). The fluorescence volume (FV, RU-nm^2/m^3) of extracts present in the atmosphere was estimated based on the EEMs at the excitation wavelength ranging from 240 to 700 nm, and then normalized it (i.e., NFV (RU-nm^2-$[mg/L]^{-1}$)) by dividing the FV with the concentration of WSOC and WIOC in the aerosol [mg m^{-3}]).

Various types of chromophores present in the $PM_{2.5}$ samples were classified and identified based on the PARAFAC analysis of the EEMs using the SOLO, the data analysis software. PARAFAC analysis was performed for each extraction fluid in each season. Ultimately, three EEM components were determined and assigned to different types of chromophores.

Additionally, fluorescence index (FI) was determined by calculating the ratio of emission intensities at 450 nm and 500 nm after excitation at 370 nm. Contributions from local biological sources can be characterized by biological index (BIX), which was calculated using the ratio of emission intensities at 380 and 430 nm following 310 nm excitation (Gao yan and Zhang, 2018).

2.3.3 Simple forcing efficiency (SFE)

It is possible to make a rough estimate of the radiative forcing caused by aerosols using a simple forcing efficiency (SFE, W/g), which was assessed as described in the literature (Bond and Bergstrom, 2006; Deng et al., 2022):

https://doi.org/10.5194/egusphere-2023-895
Preprint. Discussion started: 20 June 2023

$$SFE = \int \frac{dS(\lambda)}{d\lambda} \tau_{atm}^{2} (1 - F_c) a_s MAE(\lambda) d\lambda$$

where dS/dλ is the solar irradiance, τ_{atm} is the atmospheric transmission (0.79), F_c is the cloud fraction (approximately 0.6), a is the surface albedo (average 0.19), β is the backscatter fraction, and MSE and MAE are the mass scattering (can be ignored) and absorption efficiency, respectively.

3 Results and discussion

3.1 Characteristics of ultraviolet light absorption of BrC

3.1.1 Absorption coefficient (Abs: Mm^{-1})

The annual and seasonal concentrations and optical properties of BrC are summarized in Table 1. Temporal variations in absorption coefficient of WSBrC and WI-MSBrC at 365 nm (i.e., $Abs_{365,\ WSBrC}$ and $Abs_{365,\ WI\text{-}MSBrC}$) together with their concentrations are depicted in Fig. 1. Averages of all measured parameters peaked in winter ($Abs_{365,\ WSBrC}$ = 10.4 ± 6.76 Mm^{-1}, $Abs_{365,\ MSBrC}$= 10.0± 5.13 Mm^{-1}), followed by a decrease to autumn and spring and the lowest in summer ($Abs_{365,\ WSBrC}$ = 1.47 ± 0.77 Mm^{-1}, $Abs_{365,\ WI\text{-}MSBrC}$= 0.74 ± 0.25 Mm^{-1}). The lower absorbance in summer might have been caused by extensive oxidation of organics and thus, the enhanced decomposition of some BrC substances, due to high solar light intensity and ambient temperatures. While the increase in the absorption coefficient of BrC in winter might be mainly due to the existence of large amounts of organic aerosols under the unfavorable meteorological conditions. The seasonal variations of Abs_{365} in Tianjin were similar to those reported in the southeastern United States, but the Abs_{365} was much higher than that (0.3–3.0 Mm^{-1} in 2007) in the southeastern United States (Hecobian et al., 2010) and that in Atlanta and Los Angeles (0.88 ± 0.71 and 0.61 ± 0.38 Mm^{-1}, respectively) in summer 2010 (Zhang et al., 2011). However, compared with the Abs_{365} of WSBrC (14.1 ± 8.5 Mm^{-1}) in winter 2016 and summer 2017 (2.1 ± 1.0Mm^{-1}) in Tianjin (Deng et al., 2022), the Abs_{365} has slightly decreased in this study. Spatially, the value and contribution of Abs_{365} in this study ($Abs_{365,\ WSBrC}$ = 10.4 Mm^{-1}, $Abs_{365,\ WI\text{-}MSBrC}$= 10.0 Mm^{-1}) in winter were higher than those reported at different locations in southern China; Nanjing ($Abs_{365,\ WSBrC}$ = 4.84 Mm^{-1}, $Abs_{365,\ MSBrC}$= 7.75 Mm^{-1}) (Xie et al., 2020), Guangzhou in autumn ($Abs_{365,\ WSBrC}$ = 8.8 Mm^{-1}) (Li et al., 2018), and Lhasa in winter ($Abs_{365,\ WSBrC}$ = 1.04 Mm^{-1}, $Abs_{365,\ MSBrC}$= 1.47 Mm^{-1}) (Zhu et al., 2018). Interestingly, the Abs_{365} in Tianjin in winter is lower than that in Beijing, Xi 'an, which are heavily polluted cities in northern China (Huang et al., 2020; Li et al., 2020b). The higher Abs_{365} in winter indicates that the light absorption of BrC in $PM_{2.5}$ may have more significant effect on the climate and the photochemical reactions in the atmosphere over Tianjin in winter than in other seasons.

https://doi.org/10.5194/egusphere-2023-895
Preprint. Discussion started: 20 June 2023

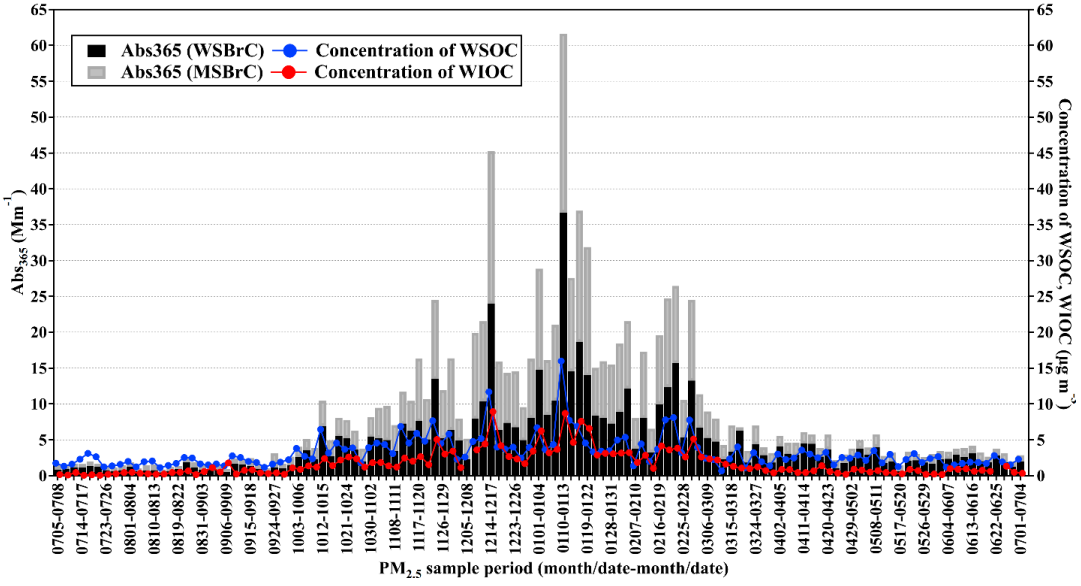

Figure 1. Time series of the light absorption coefficient of water-soluble brown carbon (WSBrC) and water-insoluble but methanol-soluble BrC (WI-MSBrC) at 365nm ($Abs_{365, WSBrC}$ and $Abs_{365, WI\text{-}MSBrC}$, respectively) and their concentrations in Tianjin, North China during 2018 and 2019.

Figure 2a shows the seasonal average absorption spectra of WSBrC and WI-MSBrC at wavelengths of 240−700 nm, which shows the common feature of BrC, i.e., the absorption of shorter wavelengths increases sharply and significantly. Such feature is different from the absorption characteristics of BC, whose AAE is close to 1 and weakly dependent on the wavelength. Another evident feature of BrC absorption spectra shown in Figure 2a is that the absorption coefficient of WI-MSBrC was always greater than that of WSBrC across the shorter wavelengths, which is consistent with the previous studies (Huang et al., 2020; Li et al., 2020b). This can be attributed to the difference in types and amounts of chromophores extracted, i.e., more chromophores were soluble in methanol (e.g., PAHs from biomass burning and fossil fuel combustion), but not in water. It is worthy to note that, π−π* electron transitions in the double bonds of aromatic compounds are the primary cause of light absorption in the wavelength range of 250−300 nm. Nitroaromatic compounds contribute 60% of absorbance in the 300−400 nm range (Hems et al., 2021). According to most of the studies, the absorption of hydroxylation and ring cleavage products formed from nitrophenol exceeds 400 nm and nitroaromatics have strong light absorption in the visible region (Vidović et al., 2020; Satish and Rastogi, 2019). The electron transitions in phenolic arenes, aniline derivatives, polyenes and polycyclic aromatic hydrocarbons with two or more rings are responsible for the absorbance in the bands between 270 and 280 nm (Baduel et al., 2009). There was a peak of light absorption at 280 nm in WI-MSBrC spectra, but not in that of WSBrC, probably because some polycyclic aromatic chromophores were insoluble in water but soluble in MeOH.

Figs. 3 and 4 show the seasonal variations in the correlations between Abs_{365} and chemical components, including WSBrC and WI-MSBrC, K^+, and Cl^-, which are possibly emitted from biomass burning. In this study, the light absorption at the wavelength of 365 nm would not be

https://doi.org/10.5194/egusphere-2023-895
Preprint. Discussion started: 20 June 2023

interfered by inorganic substances, so Abs at 365 nm was selected for analysis (Hecobian et al., 2010). High correlations were found between Abs_{365} and WSBrC, WI-MSBrC, except in summer, indicating that WSBrC and WI-MSBrC might have been derived from similar sources, except in summer, because the light absorption efficiency of organic compounds from different sources were significantly different. *For example*, precursors and reaction processes affect the light absorption capacity of SOA in the atmosphere (Zhong and Jang, 2011).

In fact, the Abs depends on the amount of BrC availability, but not of total OC content. The BrC content increases with increasing level of nitrogen containing organics (with aging in presence of NO_3^-/NH_3 etc.). So, the higher levels of OC or WSOC might occur due to enhanced primary emissions and/or secondary formation on those particular days, but the BrC content in that high amount of OC or WSOC might be less due to either aging and/or less availability of N species to produce N containing organics in summer.

https://doi.org/10.5194/egusphere-2023-895
Preprint. Discussion started: 20 June 2023

Table 1. Mass concentrations of WSOC, WIOC and absorbance efficiency of WSBrC and WI-MSBrC in $PM_{2.5}$ from Tianjin, North China.

		Spring		Summer		Autumn		Winter		Annual	
		Range	Ave ± SD	Range	Ave ± SD	Range	Ave ± SD	Range	Ave ± SD	Range	Ave ± SD
Concentrations											
WSOC (μg m^{-3})		0.69–4.03	2.48±0.82	1.14–3.12	1.88±0.53	1.16–7.68	3.45±1.71	1.37–16.0	5.06±2.99	0.69–16.0	3.25 ± 2.18
WIOC (μg m^{-3})		0.23–2.62	0.88 ± 0.63	0.00–1.33	0.43±0.32	0.21–5.07	1.55±1.04	0.00–8.93	3.74±2.09	0.00–8.93	1.68 ± 1.77
Optical parameters											
WSBrC	Abs_{365}(M m^{-1})	0.66–13.3	3.45±2.29	0.49–3.16	1.47±0.77	0.55–13.5	3.71±2.83	2.35–36.7	10.4±6.76	0.49–36.7	4.74±5.10
	MAE_{365}(m^2 g^{-1})	0.52–3.41	1.31±0.55	0.38–1.98	0.80±0.44	0.40–1.76	0.96±0.33	0.90–3.08	2.04±0.46	0.38–3.41	1.28±0.66
	$AAE_{(300–500\ nm)}$	3.85–7.57	5.42±0.74	3.90–6.88	5.17±0.83	5.12–7.99	6.21±0.65	4.50–7.39	5.88±0.58	3.85–7.99	5.66±0.82
	FI	1.13–1.63	1.37±0.09	1.16–1.49	1.31±0.07	1.36–1.61	1.47±0.07	1.29–1.44	1.37±0.02	1.13–1.63	1.38±0.09
	BIX	0.82–1.24	1.01±0.11	0.79–1.04	0.91±0.06	0.83–1.26	1.06±0.08	1.03–1.39	1.20±0.08	0.79–1.39	1.05±0.13
	HIX	1.84–3.76	2.76±0.47	2.47–3.98	3.12±0.44	2.11–4.17	3.11±0.51	1.72–3.72	2.47±0.43	1.72–4.17	2.87±0.53
	k_{365}	0.023–0.149	0.057±0.024	0.017–0.086	0.035±0.020	0.018–0.077	0.042±0.015	0.039–0.134	0.089±0.021	0.017–0.149	0.056±0.029
	$SFE_{300–400\ (W\ g^{-1})}$	0.62–2.71	1.46±0.52	0.60–2.99	1.21±0.67	0.81–5.13	1.99±0.84	1.40–4.76	3.12±0.71	0.60–5.13	1.95±1.02
	$SFE_{300–700\ (W\ g^{-1})}$	0.98–6.36	3.39±1.42	1.22–10.5	3.68±2.58	1.48–12.5	5.12±2.17	3.75–13.1	7.60±2.17	0.98–13.1	4.97±2.71
WI-MSBrC	Abs_{365}(M m^{-1})	0.44–11.3	1.99±1.95	0.40–1.26	0.74±0.25	0.32–11.0	2.83±2.51	2.85–25.0	10.0±5.13	0.32–25.0	3.87±4.69
	MAE_{365}(m^2 g^{-1})	0.42–5.81	2.41±1.28	0.89–7.05	2.50±1.78	0.18–4.70	1.86±1.02	2.01–3.42	2.69±0.36	0.18–7.05	2.36±1.26
	$AAE_{(300–500\ nm)}$	3.94–8.38	6.27±0.90	4.27–9.19	5.49±1.26	2.08–12.9	6.11±1.86	5.49–6.76	6.30±0.27	2.08–12.9	6.06±1.23
	FI	1.29–1.77	1.51±0.11	1.34–1.92	1.58±0.12	1.48–1.73	1.57±0.06	1.61–2.24	1.73±0.11	1.29–2.24	1.60±0.13
	BIX	0.94–1.76	1.23±0.18	0.92–1.65	1.32±0.18	0.83–1.36	1.05±0.14	1.20–1.62	1.43±0.09	0.83–1.76	1.26±0.21
	HIX	0.11–1.26	0.42±0.28	0.11–0.49	0.25±0.08	0.30–2.38	1.23±0.61	0.62–1.79	1.33±0.30	0.11–2.38	0.81±0.60
	k_{365}	0.018–0.253	0.105±0.057	0.039–0.307	0.109±0.079	0.008–0.205	0.081±0.045	0.0870.149	0.117±0.016	0.0010.307	0.077±0.064
	$SFE_{300–400\ (W\ g^{-1})}$	0.64–8.84	3.61±1.91	0.60–2.99	1.21±0.67	0.75–7.01	2.98±1.52	3.04–5.29	4.13±0.57	0.64–8.84	2.98±1.70
	$SFE_{300–700\ (W\ g^{-1})}$	2.48–21.8	8.70±5.03	1.22–10.5	3.68±2.58	0.92–51.3	8.69±9.23	7.06–11.7	9.36±4.51	0.92–51.3	7.58±5.75

https://doi.org/10.5194/egusphere-2023-895
Preprint. Discussion started: 20 June 2023

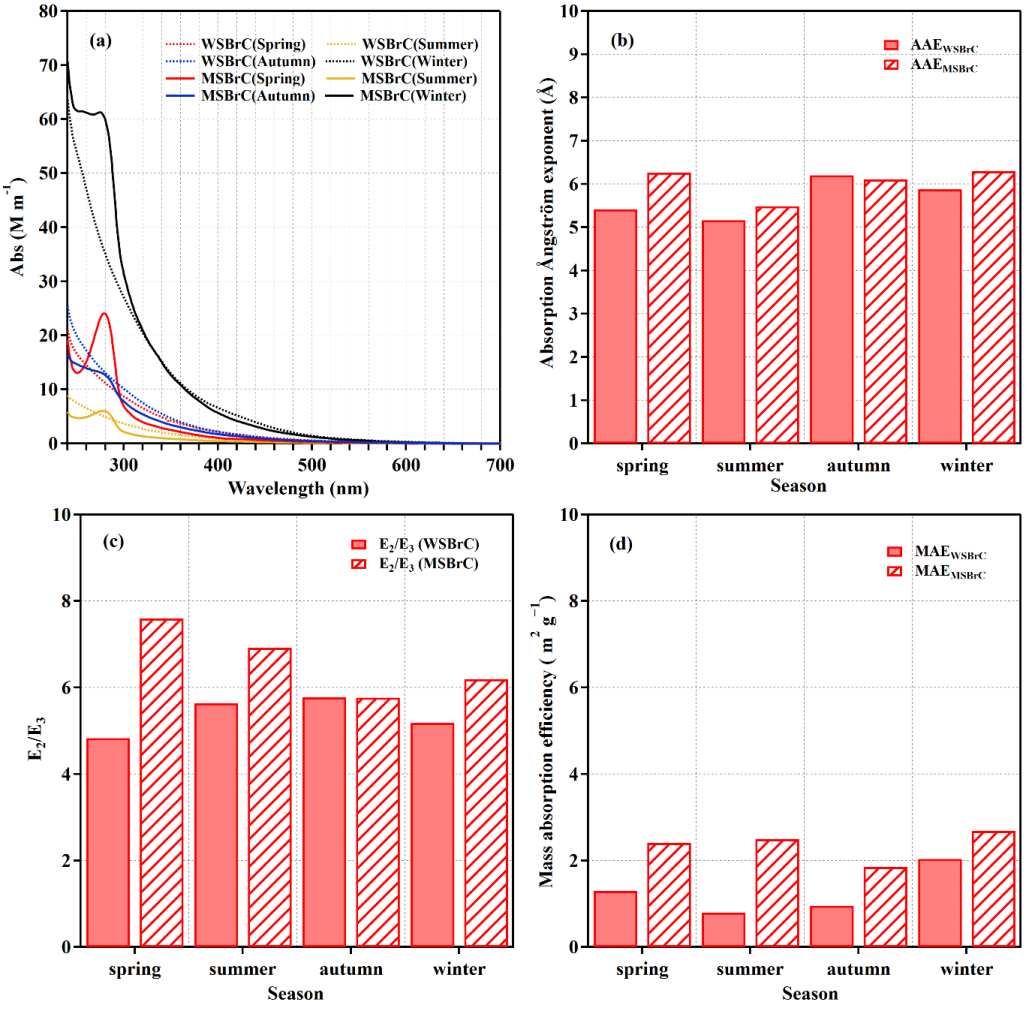

290

291 **Figure 2**. Seasonal averages of (a) absorption spectra in the wavelength range of 240–700 nm
292 plotted on a linear scale, (b) absorption Ångström exponent (AAE), (c) ratio of MAE at 250 nm to
293 that at 365 nm (E_2/E_3) and (d) mass absorption efficiency (MAE: $m^2\ g^{-1}$) of WSBrC and WI-
294 MSBrC in $PM_{2.5}$ from Tianjin, North China.

https://doi.org/10.5194/egusphere-2023-895
Preprint. Discussion started: 20 June 2023

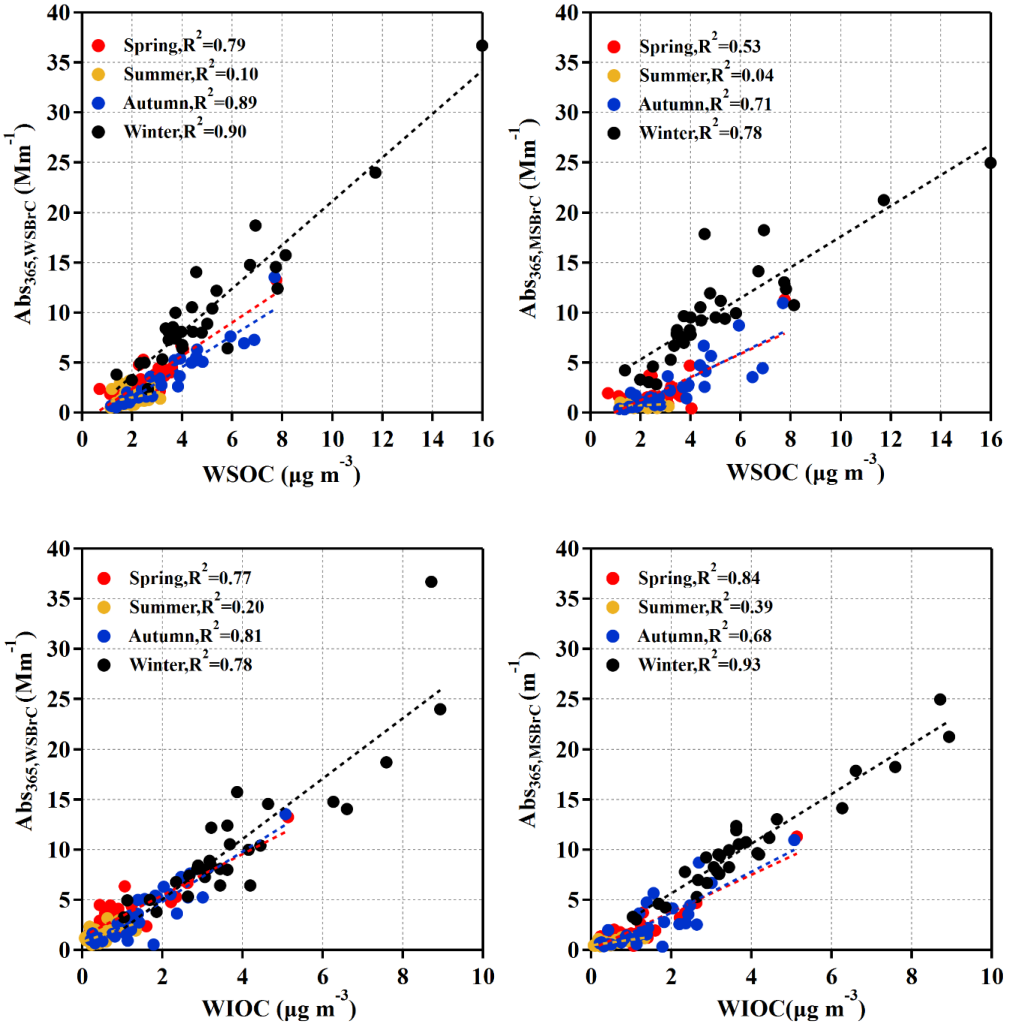

Figure 3. Scatter plots of $Abs_{365,\ WSBrC}$ and $Abs_{365,\ WI\text{-}MSBrC}$ with WSBrC and WI-MSBrC in $PM_{2.5}$ from Tianjin in each season during 2018–2019. The WSOC and WIOC data is obtained from (Dong et al., 2023).

As shown in Fig. 4, considerable positive correlations were found between Abs_{365} and K^+ and Cl^- in autumn and spring, indicating that biomass burning was a major source of BrC in those seasons. In addition, the correlation between WSOC chromophores and K^+ in autumn was stronger than that between methanol-soluble photogenic groups, which again confirmed that most of the chromophores generated by biomass burning were water-soluble photogenic groups. However, the correlation between WI-MSBrC and Cl^- was stronger than that between WSBrC and Cl^- in spring, which might be due to enhanced contribution of a large number of BrC chromophores, which were insoluble in water, from dust in spring.

https://doi.org/10.5194/egusphere-2023-895
Preprint. Discussion started: 20 June 2023

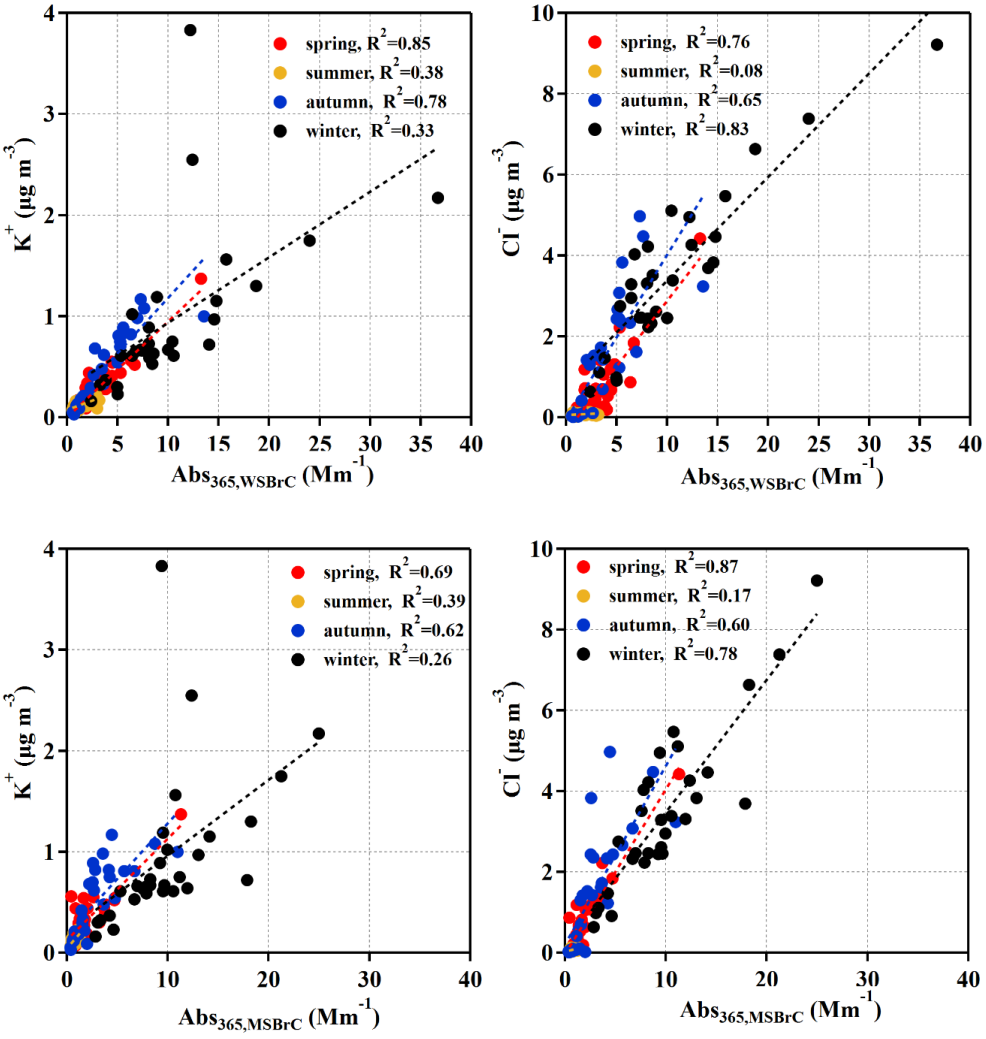

Figure 4. Scatter plots of $Abs_{365\ WSBrC}$ and $Abs_{365,\ WI\text{-}MSBrC}$ with K^+ and Cl^- in $PM_{2.5}$ from Tianjin in each season during 2018–2019. The concentration of K^+ and Cl^- from (Dong et al., 2023).

3.1.2 Absorption Ångström exponent (AAE)

The magnitude of the AAE can reflect the difference in BrC sources and atmospheric chemical processes (Lack et al., 2013). It has been reported that the AAE of light-absorbing organic species (i.e., BrC) is much larger than that of soot (BC). The AAE was found to be between 2 and 4 for the particles containing both soot and BrC. AAE value of particulate matter was closely related to its chemical composition, mixing state, particle size and other factors.

https://doi.org/10.5194/egusphere-2023-895
Preprint. Discussion started: 20 June 2023

It is important to note that the solvent extractant light absorption characteristics of organic components do not be affected by particle size and chemical composition of aerosols. The AAE value of the extract mainly depends on the types of absorbable components in the extract. Hoffer et al. (2006) isolated humic-like substances (HULIS) from particulate matter emitted by combustion substances by combining water extraction with exchange column, and measured its AAE value as 7 (Hoffer et al., 2006). As shown in Fig. 2b, the seasonal average AAE of WSBrC varied slightly between 3.85 and 7.99 with an average of 5.66, which was comparable to those reported from New Delhi, Beijing and the outflow region of northern China (Lesworth et al., 2010). The AAE of WSBrC in Tianjin was also similar to that (range, 6–8) reported in the off-line particulate matter samples collected from the southeastern United States (Hecobian et al., 2010) and downtown Atlanta (Liu et al., 2013). The AAE of WI-MSBrC (6.06 ± 1.23) was comparable with that of WSBrC, consistent with a previous study in urban Beijing during winter and Xi'an, China. It has been reported that the AAE of BrC is increased with the increase in polarity (Chen et al., 2016a). The higher AAE of the BrC implies that the OA is mostly polar in Tianjin.

3.1.3 Mass absorption efficiency (MAE: $m^2\ g^{-1}$)

The average MAE_{365} of both WSBrC and WI-MSBrC were higher in winter (1.28 and 2.36 $m^2\ g^{-1}$, respectively). It is interesting to note that minimum value of MAE_{365} of WSBrC appeared in summer (0.80 ± 0.44), which was opposite to that of WI-MSBrC, the least value was appeared in autumn (1.86 ± 1.02), which was similar with that reported in Xi'an (Li et al., 2020b). Such large seasonal differences indicated that the BrC sources might be different in each season. During winter, contributions of aerosols from coal and biomass burning were significantly higher than other seasons due to increased residential heating activities. The lower MAE_{365} values observed in summer and autumn may be attributed to biogenic sources and/or aged secondary BrC. Whereas the largest MAE_{365} appeared in cold period, which result in severe air pollution in the cold period.

3.2 Direct radiative forcing of BrC

Radiative forcing efficiency is calculated by integrating wavelengths from 300 nm to 700 nm. In this study, $SFE_{300–400}$ was integrated to estimate the radiative forcing efficiency of BrC, because the BrC strongly absorbs light in the UV range. The temporal variations of SFE in different wavelength ranges in the two solvents were shown in Fig. 5. $SFE_{300–400}$ and $SFE_{300–700}$ showed similar seasonal trend in both the solvents, which was the same as the seasonal variation of the *k*. In WSBrC, it was 61% and 52% larger in winter than those in summer, respectively, indicating that BrC abundance and strong light absorption capacity in winter led to a significant increase in direct radiative forcing of the BrC. The integrated average SFE for 300–400 nm ($SFE_{300–400}$) of WSBrC and WI-MSBrC were 1.95 ± 1.02 and 2.98 ± 1.70, respectively. The average $SFE_{300–700}$ of both WSBrC (4.97 ± 2.71) and WI-MSBrC (7.58 ± 5.75) were about 2.5 times larger than that of the $SFE_{300–400}$. The SFE of WSBrC (0.98–13.1) and WI-MSBrC (0.92–51.3) in the range of 300–700 nm varied widely, which was much larger than the maximum SFE obtained in the range of 300–400 nm. Furthermore, $SFE_{300–400}$ accounted for 40% of $SFE_{300–700}$ in the two extractants, which are similar to that reported in Tianjin by Deng et al. (2022), which indicates that the light absorption by BrC in UV range play a significant role in the radiative forcing. The imaginary part (*k*) is a significant parameter indicting the direct radiative forcing of aerosols in climate model. The *k* of WSBrC and WI-MSBrC in Tianjin showed the similar variation tendency in seasons, with

https://doi.org/10.5194/egusphere-2023-895
Preprint. Discussion started: 20 June 2023

the largest value in winter with the averages of 0.089 and 0.117, respectively. The values are shown in Table 1 and the *k* of WI-MSBrC was larger than WSBrC in all seasons, which indicate that most of light-absorbing chromophores are soluble in MeOH.

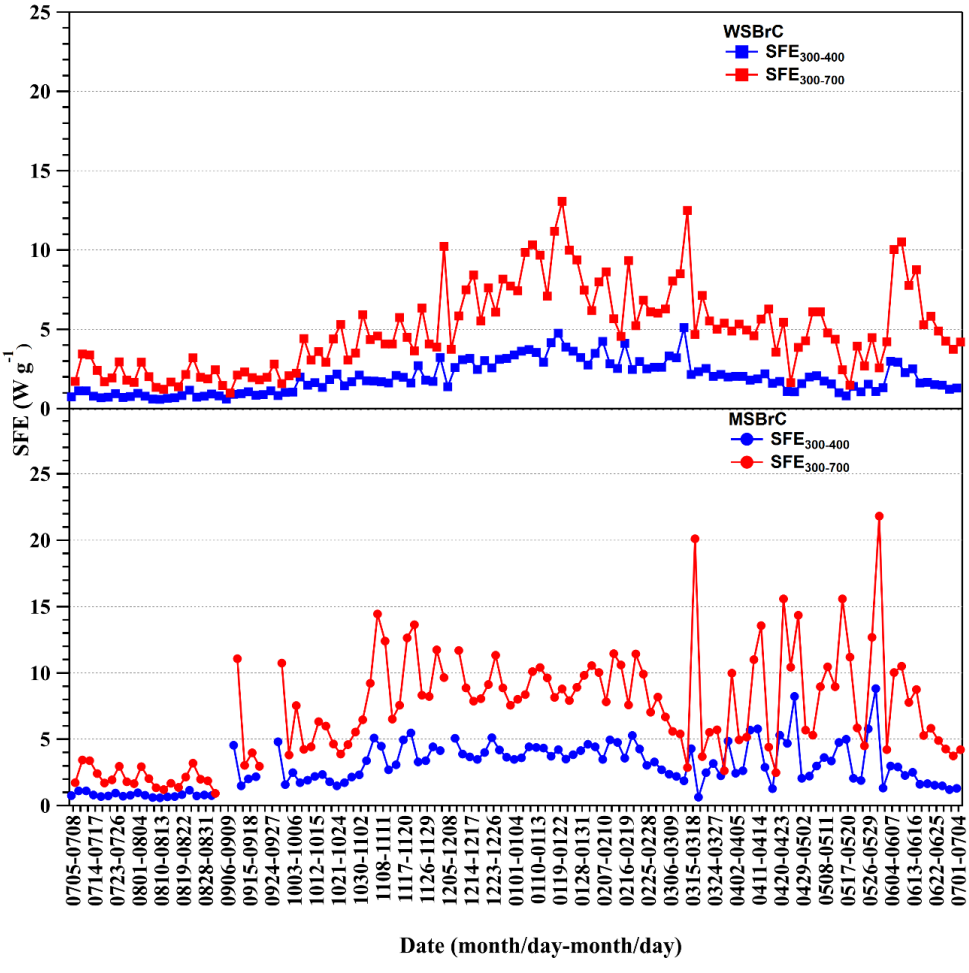

Figure 5. Temporal variations in SFE of WSBrC and WI-MSBrC from 300–400nm and 300–700nm in $PM_{2.5}$ from Tianjin.

3.3 Fluorescence characteristics of BrC

3.3.1 Fluorescent properties

The fluorescent properties of WSBrC and WI-MSBrC are presented in Table 1. The composition of chromophores in WSBrC and WI-MSBrC was analyzed by their fluorescence spectrum. By comparing the fluorescence intensity of chromophores in WSBrC and WI-MSBrC (Fig. 6), it was found that the proportion of water-soluble chromophores in Tianjin $PM_{2.5}$ was

https://doi.org/10.5194/egusphere-2023-895
Preprint. Discussion started: 20 June 2023

higher in autumn (35%), followed by summer (29%), winter (22%) and spring (22%). Previous studies have shown that biomass combustion produces more water-soluble chromophores (Budisulistiorini et al., 2017; Lin et al., 2016; Song et al., 2018). The relative content of water-soluble chromophores in Tianjin samples was higher in autumn than that in winter, suggesting that the BrC might mainly derived from biomass butning (BB) in autumn. Furthermore, the relative proportion of water-soluble chromophores in SOA is increased with the increase in oxidation degree (Updyke et al., 2012; Wong et al., 2017) and can reach up to 70% (Chen et al., 2020). The content of SOA in Tianjin was relatively high due to enhanced aging in summer. Therefore, the content of water-soluble chromophore in BrC in summer was higher than that in spring and winter. We also caculated the humification index (HIX) and fluorescence index (FI), which further supported that the water-soluble chromophores of BrC were significantly influenced by primary emissions in autumn and the aging in summer.

The fluorescence spectrum of WSBrC was similar to that of HULIS, and the humification index (HIX) is measured to reflect the degree of humification of the OA. It has been established that HIX and aromaticity show a consistent change law, that is, the value of HIX is higher, the substance has a high polycondensation degree (Deng et al., 2022). The average HIX of WSBrC and WI-MSBrC were 2.87 ± 0.53 (1.72−4.17) and 0.81 ± 0.60 (0.11−2.38) respectively, which indicate that the BrC in Tianjin might be either humified or aromatic, more apparently soluble in water. Besides, the temporal variation of HIX of WSBrC was completely different to that of WI-MSBrC. The higher molecular weight and aromatic organic compounds contribute more to WSBrC in summer and autumn while the contents of WI-MSBrC (winter > autumn > spring > summer) were opposite. This phenomenon was comparable to that in Nanjing (WSOC: 7.07 ± 2.41; MSOC: 4.84 ± 2.47) (Xie et al., 2020). This phenomenon demonstrates that the influence of molecular composition on changes in optical properties. Interestingly, it has been reported that aging processes and HIX have a significant relation (Deng et al., 2022). HIX of WSBrC confirms the BrC was significantly produced from aromatic compounds and subjected for significant atmospheric aging in summer.

Fluorescence index (FI) plays an important role in exploring the source and aging of OA and attracted much attention in recent times (Xie et al., 2020; Gao yan and Zhang, 2018; Qin et al., 2018; Deng et al., 2022). On the other hand, FI has been considered as an indicator to assess the terrestrially derived fulvic acids contribution to OA, the FI lower than 1.4 is associated with higher aromaticity (Gao yan and Zhang, 2018). The FI of WSBrC ranged from 1.13 to 1.63 with an average of 1.38, which was comparable to that reported from Lanzhou, China (1.2 in summer and 1.7 in winter) (Gao yan and Zhang, 2018). Both FI and BIX of WSBrC in autumn have higher values, indicating that the BrC was mainly derived from terrestrial organic matter that should have largely consist of aromatic compounds. On the other hand, the variation of FI was related to photobleaching. With the increase of aromatic substances during the aging of OA, FI decreased with light strength. In contrast, the FI of WI-MSBrC ranged from 1.29 to 2.24 (ave. 1.60), with the lowest in spring (1.51 ± 0.11) and the highest in winter (1.73 ± 0.11), which were higher than that of WSBrC. The variation of HIX and FI of WSBrC and WI-MSBrC indicated that the fluorescence substance contains mainly aromatic species and significantly subjected for the aging in summer, whereas in autumn, that must have mainly derived from terrestrial organics, which were highly water-soluble.

The BIX showed an obvious seasonal variations and the average value was 1.20 ± 0.08 for WSBrC and 1.43 ± 0.09 for WI-MSBrC in Tianjin $PM_{2.5}$, which were higher than those reported in the forest environment (1.01 ± 0.23) (Zhao et al., 2019). Furthermore, the BIX of WSBrC in

https://doi.org/10.5194/egusphere-2023-895
Preprint. Discussion started: 20 June 2023

Tianjin $PM_{2.5}$ was 1.20 ± 0.08 (1.03−1.39) in winter, 1.06 ± 0.08 (0.83−1.26) in autumn, 1.01 ± 0.11 (0.82−1.24) in spring and 0.91 ± 0.06 (0.79−1.04) in summer. Whereas the BIX of WI-MSBrC peaked in winter (1.43 ± 0.09) and showed the minimum value d in autumn (1.05 ± 0.14). The slightly rise in summer indicated that biological OM was more soluble in MeOH, which was different from BrC contributed by biological matter in autumn. Such results indicate that the chromophoros generated by primary sources in autumn were mostly soluble in water, while the chromophoros generated in summer were mostly water-insoluble, which was closely related to their molecular structure. Fig. 7 shows the seasonal variations of HIX, BIX and FI in WSBrC and WI-MSBrC.

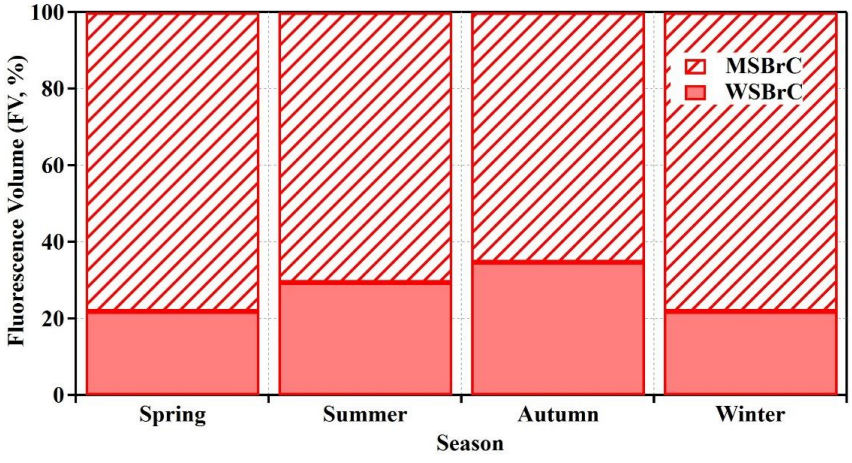

Figure 6. Relative contributions of the fluorescent volumes of the WSBrC and WI-MSBrC in $PM_{2.5}$ from Tianjin.

https://doi.org/10.5194/egusphere-2023-895
Preprint. Discussion started: 20 June 2023

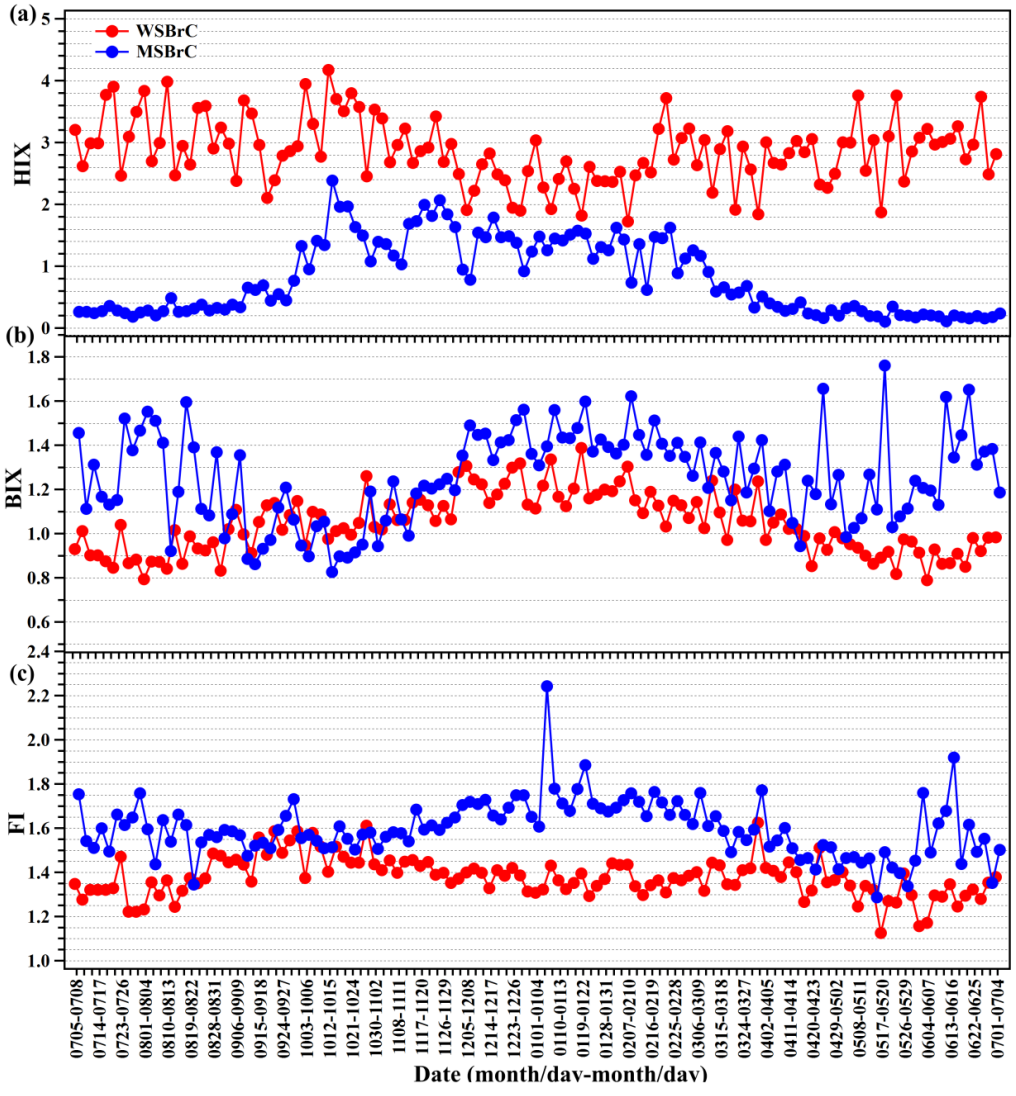

Figure 7. Temporal variations in light absorption and fluorescence properties of BrC in $PM_{2.5}$ Tianjin: (a) HIX, (b) BIX, and (c) FI.

3.3.2 Chromophore identification

It has been reported that chromophores with different excitation emission wavelengths can distinguish the types and sources of chromophores, but the types and sources of a large number of chromophores have not been determined due to their complex chemical composition and sources. Here, we successfully separated several fluorescence components from the EEM data using the parallel factor analysis (PARAFAC) method, and the results are shown in Fig. 8. The fact of the

https://doi.org/10.5194/egusphere-2023-895
Preprint. Discussion started: 20 June 2023

value of core consistency is close to 100 in PARAFAC indicates that the more the individual components that are analyzed together, the more they make up 100% of the mixture, with no unexplained residues. The core consistency of BrC extract in water was 89%, but the value can reach 95% together with that in MeOH.

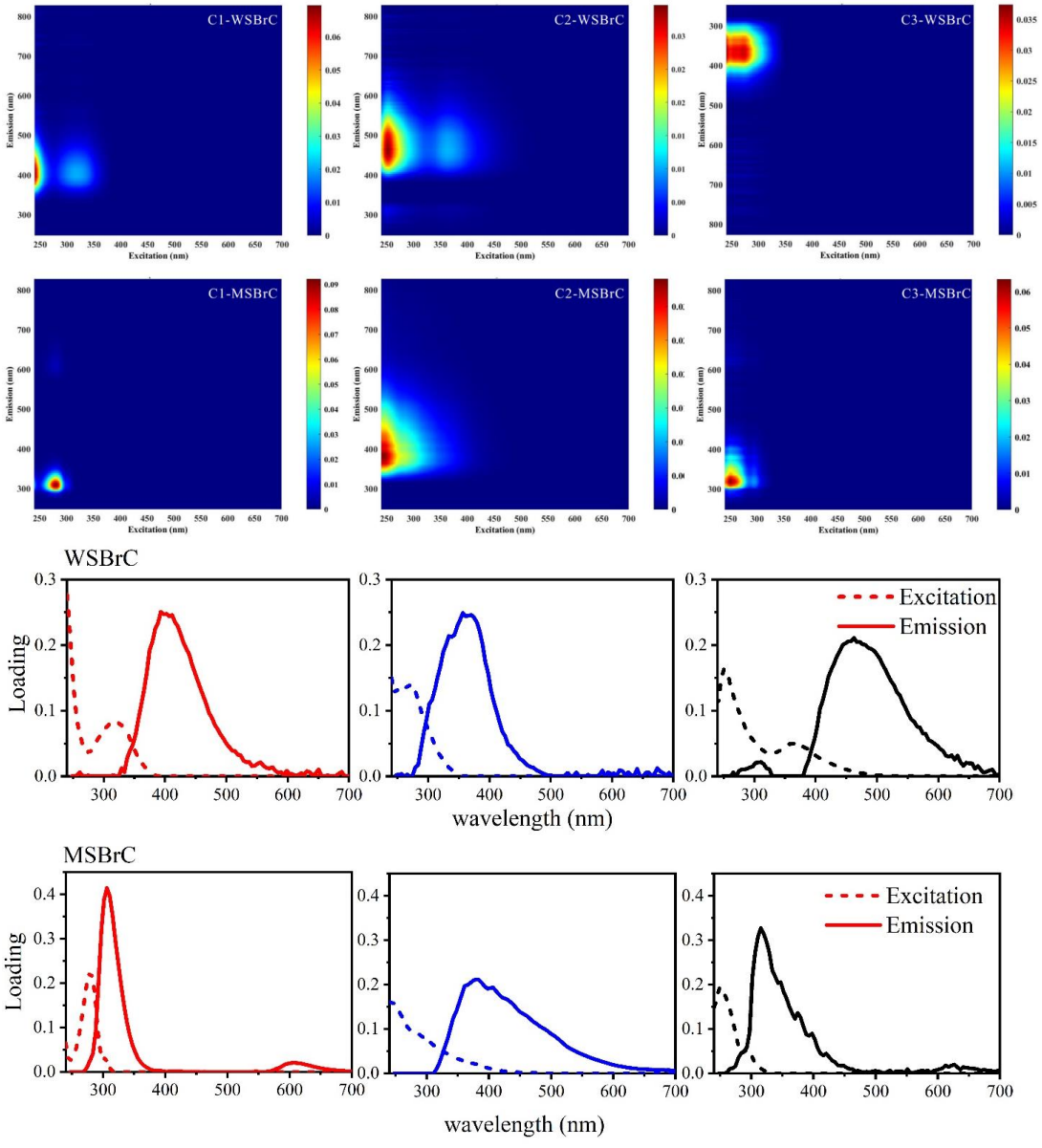

Figure 8. Three-dimensional excitation-emission matrix of three fluorescent components with emission and excitation spectra of each fluorescent component at peak emission and excitation wavelengths in WSBrC (above) and WI-MSBrC (below) obtained by PARAFAC model analysis.

https://doi.org/10.5194/egusphere-2023-895
Preprint. Discussion started: 20 June 2023

A total of three types of chromophores, two with fluorescence characteristics similar to those of humic-like substances (less oxygenated HULIS and highly oxygenated HULIS) and one with fluorescence characteristics similar to those of protein compounds (PLOM), were identified in Tianjin $PM_{2.5}$ by PARAFAC for EEMs. The types of chromophores obtained in this study together with those from the literature are summarized in Table 2. Chromophore C1 in WSBrC has a primary fluorescence peak at excitation/emission (Ex/Em): <240/393 nm, and a secondary fluorescence peak at Ex/Em: 318/393 nm. C1 can be classified as a humus-like chromophore because the bimodal distribution of the fluorescence spectrum is usually associated with humic-like substances (HULIS). The emission wavelength of C1 was closer to the UV region than that of the second peak of C2 in WSBrC, indicating the existence of a large number of aromatic substances, conjugate systems and nonlinear ring systems (Deng et al., 2022). C2 (Ex/Em ~251, 363 nm/462 nm) was identified as a common HULIS in aerosols, with higher oxidation, aromatization, molecular weight, conjugation, and unsaturation due to its larger emission wavelength (Wen et al., 2021). The molecular weight of the fluorescent chromophore as well as its degree of conjugation tend to increase with the excitation wavelength, and such increase in size and the conjugation degree may be attributed to the presence of highly aromatic conjugated structures containing heteroatoms (Chen et al., 2019). Compared to C1 and C2, C3 also contains two peaks, with shorter wavelengths (<380 nm) emission peak, which is usually associated with PLOM such as tryptophan and tyrosine, with low aromatic properties and small molecular size.

Table 2. Description and wavelength positions of PARAFAC components in this study and other repoerts. (PLOM = protein compounds; HULIS = humic-like substances)

Category	Components	Ex(nm)	Em(nm)	Substances	References
WSBrC	C1	<240, 318	393	low-oxygenated HULIS	this study
	C2	251, 363	462	high-oxygenated HULIS	
	C3	<240, 271	356.3	PLOM, such as tryptophan and tyrosine	
WI-MSBrC	C1	<240, 279	306	PLOM, tyrosine-like	
	C2	<240	379	uncertain	
	C3	251, 294	315	PLOM, tryptophan-like	
Water-soluble BrC	C1	250, 315	396	low-oxygenated HULIS	(Deng et al., 2022)
	C2	250	465	highly-oxygenated HULIS	
	C3	250	385	low-oxygenated HULIS	
	C4	250	340	PLOM, tryptophan-like	
	C5	275	305	PLOM, tyrosine-like	
WSOC	C1	240, 315	393	low-oxygenated HULIS	(Wen et al., 2021)
	C2	245, 360	476	highly-oxygenated HULIS	
	C3	<240, 290	361	PLOM, such as tryptophan and tyrosine	
	C4	275	311	PLOM, tyrosine-like	
WSM and MSM	C1	255	415	HULIS-1 component	(Chen et al., 2019)
	C2	220	340	tryptophan-like component	
	C3	255	385	HULIS-2 component	
	C4	210	300	tyrosine-like component	
	C5	250	355	amino acid-like component	
WSOC	C1	245	410	HULIS, photodegradation of macromolecules	(Xie et al., 2020)
	C2	235	398	HULIS, aromatic and saturated compounds were presented	
	C3	250, 360	466	humic-like chromophores, more aromatic and consisted of more unsaturated compounds produced by condensation reactions	
	C4	250, 285	432	terrestrial humic-like chromophore	
MSOC	C5	<235	430	terrestrial humic-like substance, photochemical product	
	C6	275	408	low oxidation humic-like	
	C7	235, 275	372	protein-like chromophore	
	C8	260, 310	364	protein-like (tryptophan-like), may be related to PAHs	

https://doi.org/10.5194/egusphere-2023-895
Preprint. Discussion started: 20 June 2023

However, MeOH-soluble chromophore C1 might be tyrosine-like substance. C2 could be HULIS or PLOM, it's not quite certain because its emission wavelength <380nm fits the profile of PLOM, but it is also close to the emission wavelength of HULIS. While C3 is a tryptophan-like substance, which was reported to contain low aromatic and small molecular weight. In general, phenols contribute significantly to C3 chromophore as they are the products of incomplete pyrolysis of lignin and cellulose and are used as indicators of biomass burning (Wen et al., 2021). The water-insoluble chromophores of all samples in this study can be classified as PLOM. This indicates that the chromophores of protein substances mainly dissolve in solvents with high polarity. As shown in Fig. 9, the water-soluble extracts contained more HULIS. In contrast, the MeOH extracts contained more PLOM chromophores than those in the water-soluble extracts.

Surprisingly, according to the excitation emission wavelength, we classified the fluorescence component of WI-MSBrC substance as PLOM, but the correlation between their fluorescence intensity and BIX ($R^2 = 0.06$, $p < 0.05$) was very small, far lower than that of WSBrC substance and BIX ($R^2 = 0.18$, $p < 0.05$). On the contrary, the correlation between their fluorescence intensity and HIX ($R^2 = 0.54$, $p < 0.05$) was much higher than that of WSBrC ($R^2 = 0.01$, $p < 0.05$). Although PLOM may be associated with some polycyclic aromatic hydrocarbons (PAHs) or phenols from fossil fuel combustion and biomass burning, especially in urban aerosols, the correlation is puzzling.

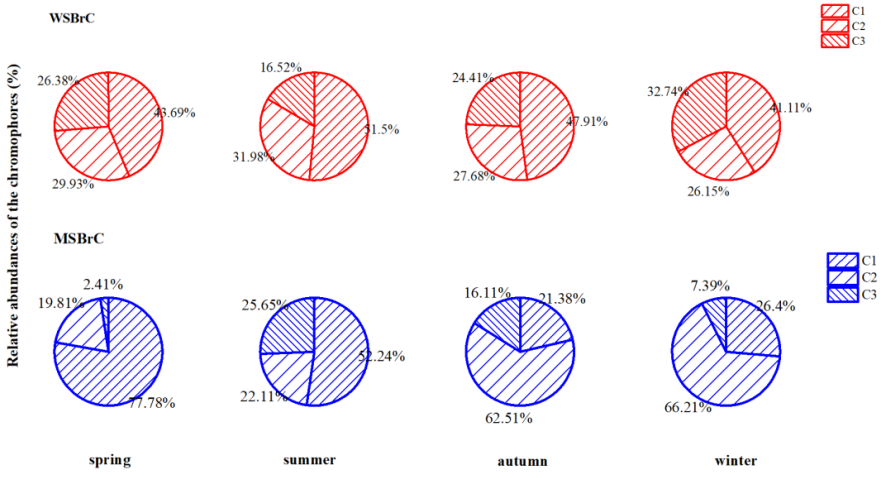

Figure 9. Relative abundances of the chromophores of the WSBrC and WI-MSBrC in $PM_{2.5}$ from Tianjin.

Fig. 9 displays the average relative contributions of the fluorescent components of WSBrC and WI-MSBrC during different periods. On average, the humic-like chromophores together contributed more than 60% to the fluorescence intensity in WSBrC, suggesting that humic-like chromophores played a dominant role in fluorescence properties of WSBrC in Tianjin. Generally, the low-oxygenated chromophores C1 made considerable contributions in each season. C2, as highly oxygenated HULIS, has a greater relative contribution in summer, which might be due to the strong solar radiation in summer, which made some HULIS with little oxygen photodegraded and form highly oxygenated HULIS through a series of oxidation reactions. In contrast, in WI-

https://doi.org/10.5194/egusphere-2023-895
Preprint. Discussion started: 20 June 2023

MSBrC, the average contribution of PLOM to fluorescence intensity was higher than 70% in spring (80.2%) and summer (77.9%), but C2 component dominated in winter and autumn. This indicated that biological activities increased in spring and summer and the relative abundance of bioaerosols was higher during that period.

3.4 Potential sources of BrC

The types of chromophores present in aerosols are numerous and their sources are complex. A chromophore may originate from a single source or may be contributed by multiple sources. To explore the potential sources of BrC, correlations of FV with chemical components and light absorption of $PM_{2.5}$ were studied. The total FVs of WSBrC and WI-MSBrC with SOC showed a significant correlation in autumn ($R^2 = 0.80$, $p < 0.05$) and spring ($R^2 = 0.52$, $p < 0.05$). Furthermore, the correlation between FVs and EC in each season was insignificant. Such relations suggest that the secondary formation processes contributed more in autumn and spring. A good correlation between FVs and Abs_{365} of WSBrC and WI-MSBrC was found in all seasons, except in winter, which indicate that most of light-absorbing materials would also have fluorescence character.

The relative contents of different chromophores in different polar extracts were also different. The results showed that the overall optical properties of the different samples were different (Fig. 10). Recently, it has been reported that the aerosols derived from biomass burning and coal combustion exhibit the highest NFV values, while SOA show the lowest NFV values (Chen et al., 2020). NFV in all samples studied in Tianjin during 2018–2019 was very similar to that of POA and higher than that of SOA. Such result reveal that the chromophores in the Tianjin $PM_{2.5}$ might mainly be derived from a primary combustion sources. In addition, the NFVs of the Tianjin $PM_{2.5}$ were higher in winter than in summer, which is likely and can be attributed to the photolysis of chromophores in summer. In addition, NFV in MeOH-soluble OC was much higher than that in WSBrC, which indicated that chromophores were abundant in WI-MSBrC than in the WSBrC. Extraction of BrC by variety of solvents is a subject of our future research.

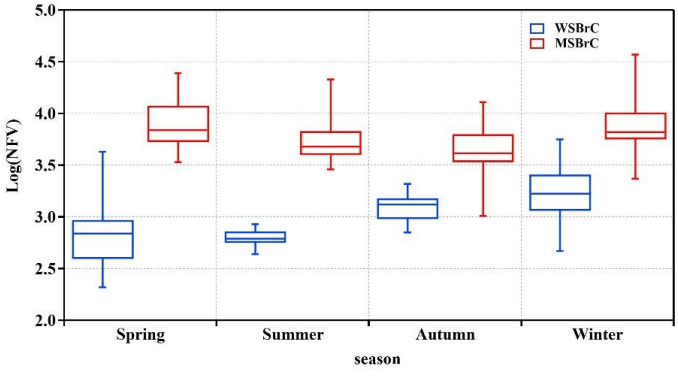

Figure 10. The normalized fluorescence volumes (NFVs) of the WSBrC and WI-MSBrC of $PM_{2.5}$ from Tianjin, North China.

In order to further identify the sources of the chromophores, the correlation between $\delta^{13}C_{TC}$ as well as $\delta^{15}N_{TN}$ and the optical parameters of BrC were analyzed. As shown in Fig.11, $\delta^{15}N_{TN}$ in Tianjin $PM_{2.5}$ showed a negative correlation with $Abs_{365,\ WSBrC}$ in autumn ($R^2 = 0.61$) and summer ($R^2 = 0.55$), whereas the $\delta^{13}C_{TC}$ showed a significant relation neither with $Abs_{365,\ WSBrC}$ nor with $Abs_{365,\ WI\text{-}MSBrC}$ in all seasons. Such relations indicated that some of N-containing substances

https://doi.org/10.5194/egusphere-2023-895
Preprint. Discussion started: 20 June 2023

derived from biomass burning emissions, biological emissions and subsequent aging of aerosols in summer and autumn might contain BrC chromophores and were soluble in water (Satish and Rastogi, 2019).

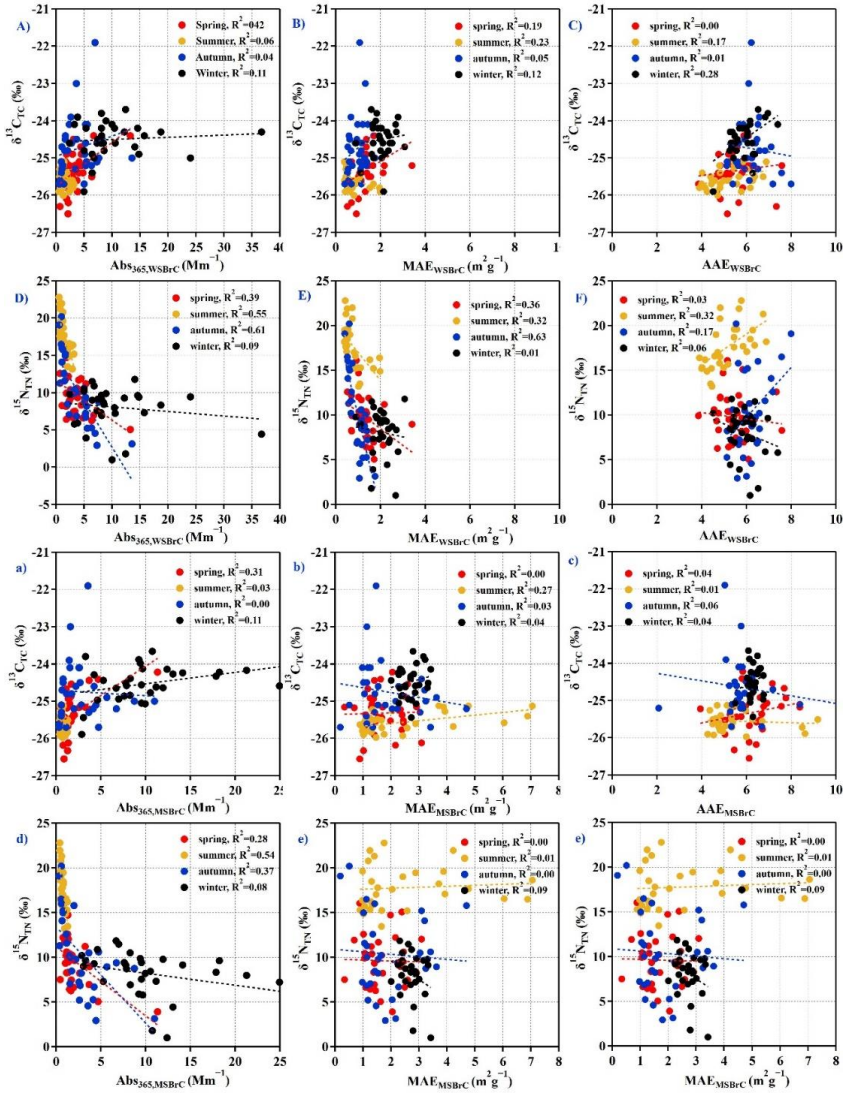

Figure 11. Scatter plots between $\delta^{13}C_{TC}/\delta^{15}N_{TN}$ and optical parameters (Abs_{365}, AAE, MAE) in WSBrC and WI-MSBrC in $PM_{2.5}$ from Tianjin. The $\delta^{13}C_{TC}/\delta^{15}N_{TN}$ data is obtained from (Dong et al., 2023).

4. Summary and Conclusions

This study presents the temporal variations in light absorption and fluorescence properties of water-soluble BrC (WSBrC) and the water-insoluble but MeOH-soluble BrC (WI-MSBrC) in

https://doi.org/10.5194/egusphere-2023-895
Preprint. Discussion started: 20 June 2023

$PM_{2.5}$ collected from Tianjin, North China during July 5, 2018 – July 5, 2019. Based on correlation between BrC and aerosol chemical composition, the possible sources of BrC were comprehensively analyzed. Light absorption properties of WSBrC and WI-MSBrC in Tianjin were investigated and found to be distinct from season to season, which was lower in spring and summer, compared with that in autumn and winter. The AAE of WI-MSBrC was comparable with that of WSBrC and indicated that Tianjin $PM_{2.5}$ contains more polar BrC. The Mass absorption efficiency of WSBrC and WI-MSBrC (MAE_{365}) exhibited distinct seasonal variations, which was higher in winter and lower in summer and autumn. Biologically derived or secondary BrC might be one of the reasons for the lower MAE_{365} values in summer and autumn. The light absorption of BrC in the range of 300–400 nm to the light absorption of WSBrC and WI-MSBrC in whole range (300–700 nm) was close to 40%, indicating that BrC plays an important role in climate warming and atmospheric photochemical reactions. In order to better assess its impact on climate, further work is needed through observations and laboratory simulations of BrC generation and aging.

In addition, based on PARAFAC analysis model, EEM data were comprehensively analyzed to compare the types and abundance of different color clusters in different aerosol samples, and a portion of source of BrC chromophore was determined by different excitation-emission wavelengths. In this study, BrC chromophore was divided into three categories: low-oxygenated HULIS, high-oxygenated HULIS and protein-like compound (PLOM). The high-oxygenated HULIS was more reactive than other categories in the atmospheric photooxidation. By comparing the fluorescence fluxes of different polar extraction solutions, it was found that WI-MSBrC substances contributed more than half of the fluorescence, indicating that there were more polar BrC substances in Tianjin aerosol, which attributed from anthropogenic emissions. The correlation between BrC optical properties and aerosol chemical composition indicated that fossil fuel combustion significantly contributed to BrC content in winter, while primary biological emission and aging reaction significantly contributed to the BrC content in summer. These results illustrated the light absorption properties of BrC in metropolis aerosols and emphasized its significant contribution to radiative forcing.

Declaration of competing intertest

The authors declare no competing intertest in this paper.

Data Availability Statement

The data used in this study can be found online at https://doi.org/10.5281/zenodo.7316371 (Dong et al., 2022), and at https://doi.org/10.5281/zenodo.5140861 (Dong et al., 2021).

Acknowledgments

This work was supported in part by National Natural Science Foundation of China (Grant No. 41775120 and 42277090) & National Key Research and Development Plan (Grant No. 2017YFC0212700), China. The author also thanks to Mr. Yunting Xiao's help for writing a code to calculate the SFE.

https://doi.org/10.5194/egusphere-2023-895
Preprint. Discussion started: 20 June 2023

Author contribution

ZD and CMP conceptualized this study. ZD and PL conducted the sampling. ZD conducted the chemical analyses, interpreted the data and wrote the manuscript. CMP supervised the research and acquired the funding for this study. XZ, ZXY and ZXM administrated the project. CMP, ZX, DJ, PF and CQL contributed in discussing the results and review and editing the manuscript.

References

Andreae, M. O., and Gelencs´er, A.: Black carbon or brown carbon? The nature of light-absorbing carbonaceous aerosols, Atmospheric Chemistry and Physics, 6, 3131–3148, www.atmos-chem-phys.net/6/3131/2006/, 2006.

Baduel, C., Voisin, D., and Jaffrezo, J. L.: Comparison of analytical methods for Humic Like Substances (HULIS) measurements in atmospheric particles, Atmospheric Chemistry and Physics, 9, 5949-5962, 10.5194/acp-9-5949-2009, 2009.

Bond, T. C., and Bergstrom, R. W.: Light absorption by carbonaceous particles: An investigative review, Aerosol Science and Technology, 40, 27-67, 10.1080/02786820500421521, 2006.

Brown, H., Liu, X., Pokhrel, R., Murphy, S., Lu, Z., Saleh, R., Mielonen, T., Kokkola, H., Bergman, T., Myhre, G., Skeie, R. B., Watson-Paris, D., Stier, P., Johnson, B., Bellouin, N., Schulz, M., Vakkari, V., Beukes, J. P., van Zyl, P. G., Liu, S., and Chand, D.: Biomass burning aerosols in most climate models are too absorbing, Nature Communications, 12, 277, 10.1038/s41467-020-20482-9, 2021.

Budisulistiorini, S. H., Riva, M., Williams, M., Chen, J., Itoh, M., Surratt, J. D., and Kuwata, M.: Light-absorbing brown carbon aerosol constituents from combustion of indonesian peat and biomass, Environmental Science & Technology, 51, 4415-4423, 10.1021/acs.est.7b00397, 2017.

Cao, T., Li, M., Xu, C., Song, J., Fan, X., Li, J., Jia, W., and Peng, P.: Technical note: Identification of chemical composition and source of fluorescent components in atmospheric water-soluble brown carbon by excitation-emission matrix with parallel factor analysis: Potential limitation and application, Atmospheric Chemistry and Physics Discussions, 2022, 1-41, 10.5194/acp-2022-676, 2022.

Chakrabarty, R. K., Moosmuller, H., Chen, L. W. A., Lewis, K., Arnott, W. P., Mazzoleni, C., Dubey, M. K., Wold, C. E., Hao, W. M., and Kreidenweis, S. M.: Brown carbon in tar balls from smoldering biomass combustion, Atmospheric Chemistry and Physics 10, 6363-6370, 10.5194/acp-10-6363-2010, 2010.

Chen, Q., Fumikazu, I., Hayato, H., Daichi, A., and Michihiro, M.: Chemical structural characteristics of HULIS and other fractionated organic matter in urban aerosols: Results from mass spectral and FT-IR analysis, Environmental Science & Technology, 50, 1721-1730, 10.1021/acs.est.5b05277, 2016a.

Chen, Q., Miyazaki, Y., Kawamura, K., Matsumoto, K., Coburn, S., Volkamer, R., Iwamoto, Y., Kagami, S., Deng, Y., Ogawa, S., Ramasamy, S., Kato, S., Ida, A., Kajii, Y., and Mochida, M.: Characterization of chromophoric water-soluble organic matter in urban, forest, and marine aerosols by HR-ToF-AMS analysis and excitation–emission matrix spectroscopy, Environmental Science & Technology, 50, 10351-10360, 10.1021/acs.est.6b01643, 2016b.

Chen, Q., Mu, Z., Song, W., Wang, Y., Yang, Z., Zhang, L., and Zhang, Y.-L.: Size-resolved characterization of the chromophores in atmospheric particulate matter from a typical coal-burning city in China, Journal of Geophysical Research: Atmospheres, 124, 10546-10563, https://doi.org/10.1029/2019JD031149, 2019.

Chen, Q., Li, J., Hua, X., Jiang, X., Mu, Z., Wang, M., Wang, J., Shan, M., Yang, X., Fan, X., Song, J., Wang, Y., Guan, D., and Du, L.: Identification of species and sources of atmospheric chromophores by fluorescence excitation-emission matrix with parallel factor analysis, Science of the Total Environment, 718, 137322, 10.1016/j.scitotenv.2020.137322, 2020.

Corbin, J. C., Czech, H., Massabò, D., de Mongeot, F. B., Jakobi, G., Liu, F., Lobo, P., Mennucci, C., Mensah, A. A., Orasche, J., Pieber, S. M., Prévôt, A. S. H., Stengel, B., Tay, L. L., Zanatta, M., Zimmermann, R., El Haddad, I., and Gysel, M.: Infrared-absorbing carbonaceous tar can dominate light absorption by marine-engine exhaust, npj Climate and Atmospheric Science, 2, 12, 10.1038/s41612-019-0069-5, 2019.

Deng, J., Ma, H., Wang, X., Zhong, S., Zhang, Z., Zhu, J., Fan, Y., Hu, W., Wu, L., Xiaodong, L., Ren, L., Pavuluri, C. M., Pan, X., Sun, Y., Wang, Z., Kawamura, K., and Fu, P.: Measurement Report: Optical properties and sources of water-soluble brown carbon in Tianjin, North China: insights from organic molecular compositions, Atmospheric Chemistry and Physics, 22, 6449-6470, 10.5194/acp-2021-1045, 2022.

https://doi.org/10.5194/egusphere-2023-895
Preprint. Discussion started: 20 June 2023

Diggs, D. L., Huderson, A. C., Harris, K. L., Myers, J. N., Banks, L. D., Rekhadevi, P. V., Niaz, M. S., and Ramesh, A.: Polycyclic aromatic hydrocarbons and digestive tract cancers: a perspective, Journal of Environmental Science and Health, Part C, 29, 324-357, 10.1080/10590501.2011.629974, 2011.
Dong, Z., Pavuluri, C. M., Xu, Z., Wang, Y., Li, P., Fu, P., and Liu, C. Q.: Measurement report: Chemical components and 13C and 15N isotope ratios of fine aerosols over Tianjin, North China: year-round observations, Atmospheric Chemistry and Physics, 23, 2119-2143, 10.5194/acp-23-2119-2023, 2023.
Dong, Z. C., Pavuluri, C. M., Xu, Z. J., Wang, Y., Li, P. S., Fu, P. Q., and Liu, C. Q.: Year-round observations of bulk components and 13C and 15N isotope ratios of fine aerosols at Tianjin, North China – Data set. 2021.
Dong, Z. C., Pavuluri, C. M., Li, P. S., Xu, Z. J., Deng, J. J., Zhao, X. Y., and Zhao, X. M.: Year-round observations of the optical properties of brown carbon in fine aerosols at Tianjin, North China – Data set. 2022.
Feng, Y., Ramanathan, V., and Kotamarthi, V. R.: Brown carbon: a significant atmospheric absorber of solar radiation?, Atmospheric Chemistry and Physics Discussions, 10.5194/acpd-13-2795-2013, 10.5194/acpd-13-2795-2013, 2013.
Gao yan, and Zhang, y.: Formation and photochemical investigation of brown carbon by hydroxyacetone reactions with glycine and ammonium sulfate, Royal Society of Chemistry Advances, 8, 20719-20725, 10.1039/C8RA02019A, 2018.
Gu, Q., and Kenny, J. E.: Improvement of inner filter effect correction based on determination of effective geometric parameters using a conventional fluorimeter, Analytical Chemistry, 81, 420-426, 10.1021/ac801676j, 2009.
Hecobian, A., Zhang, X., Zheng, M., Frank, N., Edgerton, E. S., and Weber, R. J.: Water-Soluble Organic Aerosol material and the light-absorption characteristics of aqueous extracts measured over the Southeastern United States, Atmospheric Chemistry and Physics, 10, 5965-5977, 10.5194/acp-10-5965-2010, 2010.
Hems, R. F., Schnitzler, E. G., Liu-Kang, C., Cappa, C. D., and Abbatt, J. P. D.: Aging of atmospheric brown carbon aerosol, ACS Earth and Space Chemistry, 5, 722-748, 10.1021/acsearthspacechem.0c00346, 2021.
Hoffer, A., Gelencsér, A., Guyon, P., Kiss, G., Schmid, O., Frank, G. P., Artaxo, P., and Andreae, M. O.: Optical properties of humic-like substances (HULIS) in biomass-burning aerosols, Atmospheric Chemistry and Physics, 6, 3563-3570, 10.5194/acp-6-3563-2006, 2006.
Huang, R. J., Yang, L., Cao, J., Chen, Y., Chen, Q., Li, Y., Duan, J., Zhu, C., Dai, W., Wang, K., Lin, C., Ni, H., Corbin, J. C., Wu, Y., Zhang, R., Tie, X., Hoffmann, T., O'Dowd, C., and Dusek, U.: Brown carbon aerosol in urban Xi'an, Northwest China: The composition and light absorption properties, Environmental Science & Technology, 52, 6825-6833, 10.1021/acs.est.8b02386, 2018.
Huang, R. J., Yang, L., Shen, J., Yuan, W., Gong, Y., Guo, J., Cao, W., Duan, J., Ni, H., Zhu, C., Dai, W., Li, Y., Chen, Y., Chen, Q., Wu, Y., Zhang, R., Dusek, U., O'Dowd, C., and Hoffmann, T.: Water-insoluble organics dominate brown carbon in wintertime urban aerosol of China: Chemical characteristics and optical properties, Environmental Science & Technology, 54, 7836-7847, 10.1021/acs.est.0c01149, 2020.
Izhar, S., Gupta, T., and Panday, A. K.: Improved method to apportion optical absorption by black and brown carbon under the influence of haze and fog at Lumbini, Nepal, on the Indo-Gangetic Plains, Environmental Pollution, 263, 114640, https://doi.org/10.1016/j.envpol.2020.114640, 2020.
Jacobson, M. Z.: Isolating nitrated and aromatic aerosols and nitrated aromatic gases as sources of ultraviolet light absorption, Journal of Geophysical Research-Atmospheres, 104, 3527-3542, 10.1029/1998jd100054, 1999.
Jo, D. S., Park, R. J., Lee, S., Kim, S. W., and Zhang, X.: A global simulation of brown carbon: implications for photochemistry and direct radiative effect, Atmospheric Chemistry and Physics, 16, 3413-3432, 10.5194/acp-16-3413-2016, 2016.
Kasthuriarachchi, N. Y., Rivellini, L.-H., Chen, X., Li, Y. J., and Lee, A. K. Y.: Effect of relative humidity on secondary brown carbon formation in aqueous droplets, Environmental Science & Technology, 54, 13207-13216, 10.1021/acs.est.0c01239, 2020.
Lack, D. A., Bahreni, R., Langridge, J. M., Gilman, J. B., and Middlebrook, A. M.: Brown carbon absorption linked to organic mass tracers in biomass burning particles, Atmospheric Chemistry and Physics, 13, 2415-2422, 10.5194/acp-13-2415-2013, 2013.
Laskin, A., Laskin, J., and Nizkorodov, S. A.: Chemistry of atmospheric brown carbon, Chemical Reviews, 115, 4335-4382, 10.1021/cr5006167, 2015.
Lawaetz, A. J., and Stedmon, C. A.: Fluorescence intensity calibration using the Raman scatter peak of water, Applied Spectroscopy, 63, 936-940, 10.1366/000370209788964548, 2009.
Lesworth, T., Baker, A. R., and Jickells, T.: Aerosol organic nitrogen over the remote Atlantic Ocean, Atmospheric Environment, 44, 1887-1893, https://doi.org/10.1016/j.atmosenv.2010.02.021, 2010.

https://doi.org/10.5194/egusphere-2023-895
Preprint. Discussion started: 20 June 2023

690 Li, C., He, Q., Hettiyadura, A. P. S., Käfer, U., Shmul, G., Meidan, D., Zimmermann, R., Brown, S. S., George, C.,
691 Laskin, A., and Rudich, Y.: Formation of secondary brown carbon in biomass burning aerosol proxies through NO3
692 radical reactions, Environmental Science & Technology, 54, 1395-1405, 10.1021/acs.est.9b05641, 2020a.
693 Li, J., Zhang, Q., Wang, G., Li, J., Wu, C., Liu, L., Wang, J., Jiang, W., Li, L., Ho, K. F., and Cao, J.: Optical
694 properties and molecular compositions of water-soluble and water-insoluble brown carbon (BrC) aerosols in
695 northwest China, Atmospheric Chemistry and Physics, 20, 4889-4904, 10.5194/acp-20-4889-2020, 2020b.
696 Li, S., Zhu, M., Yang, W. Q., Tang, M. J., Huang, X. L., Yu, Y. G., Fang, H., Yu, X., Yu, Q. Q., Fu, X. X., Song,
697 W., Zhang, Y. L., Bi, X. H., and Wang, X. M.: Filter-based measurement of light absorption by brown carbon in
698 PM2.5 in a megacity in South China, Science of the Total Environment, 633, 1360-1369,
699 10.1016/j.scitotenv.2018.03.235, 2018.
700 Li, X., Fu, P., Tripathee, L., Yan, F., Hu, Z., Yu, F., Chen, Q., Li, J., Chen, Q., Cao, J., and Kang, S.: Molecular
701 compositions, optical properties, and implications of dissolved brown carbon in snow/ice on the Tibetan Plateau
702 glaciers, Environment International, 164, 107276, https://doi.org/10.1016/j.envint.2022.107276, 2022.
703 Lin, G., Penner, J. E., Flanner, M. G., Sillman, S., Xu, L., and Zhou, C.: Radiative forcing of organic aerosol in the
704 atmosphere and on snow: Effects of SOA and brown carbon, Journal of Geophysical Research: Atmospheres, 119,
705 7453-7476, 10.1002/2013jd021186, 2014.
706 Lin, P., Aiona, P. K., Li, Y., Shiraiwa, M., Laskin, J., Nizkorodov, S. A., and Laskin, A.: Molecular characterization
707 of brown carbon in biomass burning berosol particles, Environmental Science & Technology, 50, 11815-11824,
708 10.1021/acs.est.6b03024, 2016.
709 Liu, J., Bergin, M., Guo, H., King, L., Kotra, N., Edgerton, E., and Weber, R. J.: Size-resolved measurements of
710 brown carbon in water and methanol extracts and estimates of their contribution to ambient fine-particle light
711 absorption, Atmospheric Chemistry and Physics, 13, 12389-12404, 10.5194/acp-13-12389-2013, 2013.
712 Liu, J., Scheuer, E., Dibb, J., Diskin, G. S., Ziemba, L. D., Thornhill, K. L., Anderson, B. E., Wisthaler, A.,
713 Mikoviny, T., Devi, J. J., Bergin, M., Perring, A. E., Markovic, M. Z., Schwarz, J. P., Campuzano-Jost, P., Day, D.
714 A., Jimenez, J. L., and Weber, R. J.: Brown carbon aerosol in the North American continental troposphere: sources,
715 abundance, and radiative forcing, Atmospheric Chemistry and Physics, 15, 7841-7858, 10.5194/acp-15-7841-2015,
716 2015.
717 Murphy, K. R., Stedmon, C. A., Graeber, D., and Bro, R.: Fluorescence spectroscopy and multi-way techniques.
718 PARAFAC, Analytical Methods, 5, 6557-6566, 10.1039/C3AY41160E, 2013.
719 Park, R. J., Kim, M. J., Jeong, J. I., Youn, D., and Kim, S.: A contribution of brown carbon aerosol to the aerosol
720 light absorption and its radiative forcing in East Asia, Atmospheric Environment, 44, 1414-1421,
721 10.1016/j.atmosenv.2010.01.042, 2010.
722 Peters, S., Talaska, G., Jonsson, B. A., Kromhout, H., and Vermeulen, R.: Polycyclic aromatic hydrocarbon
723 exposure, urinary mutagenicity, and DNA adducts in rubber manufacturing workers, Cancer Epidemiol Biomarkers
724 Prev, 17, 1452-1459, 10.1158/1055-9965.EPI-07-2777, 2008.
725 Qin, J., Zhang, L., Zhou, X., Duan, J., Mu, S., Xiao, K., Hu, J., and Tan, J.: Fluorescence fingerprinting properties
726 for exploring water-soluble organic compounds in PM2.5 in an industrial city of northwest China, Atmospheric
727 Environment, 184, 203-211, https://doi.org/10.1016/j.atmosenv.2018.04.049, 2018.
728 Rizzo, L. V., Correia, A. L., Artaxo, P., Procópio, A. S., and Andreae, M. O.: Spectral dependence of aerosol light
729 absorption over the Amazon Basin, Atmospheric Chemistry and Physics, 11, 8899-8912, 10.5194/acp-11-8899-
730 2011, 2011.
731 Rizzo, L. V., Artaxo, P., Müller, T., Wiedensohler, A., Paixão, M., Cirino, G. G., Arana, A., Swietlicki, E., Roldin,
732 P., Fors, E. O., Wiedemann, K. T., Leal, L. S. M., and Kulmala, M.: Long term measurements of aerosol optical
733 properties at a primary forest site in Amazonia, Atmos. Chem. Phys., 13, 2391-2413, 10.5194/acp-13-2391-2013,
734 2013.
735 Sareen, N., N., S. A., L., S. E., D., M., and F., M. V.: Secondary organic material formed by methylglyoxal in
736 aqueous aerosol mimics, Atmospheric Chemistry and Physics, 10, 997–1016, www.atmos-chem-
737 phys.net/10/997/2010/, 2010.
738 Satish, R., and Rastogi, N.: On the use of brown carbon spectra as a tool to understand their broader composition
739 and characteristics: A case study from crop-residue burning samples, American Chemical Society Omega, 4, 1847-
740 1853, 10.1021/acsomega.8b02637, 2019.
741 Song, J., Li, M., Jiang, B., Wei, S., Fan, X., and Peng, P.: Molecular characterization of water-soluble Humic like
742 substances in smoke particles emitted from combustion of biomass materials and coal using Ultrahigh-Resolution
743 Electrospray Ionization Fourier Transform Ion Cyclotron Resonance Mass Spectrometry, Environmental Science &
744 Technology, 52, 2575-2585, 10.1021/acs.est.7b06126, 2018.

https://doi.org/10.5194/egusphere-2023-895
Preprint. Discussion started: 20 June 2023

Updyke, K. M., Nguyen, T. B., and Nizkorodov, S. A.: Formation of brown carbon via reactions of ammonia with secondary organic aerosols from biogenic and anthropogenic precursors, Atmospheric Environment, 63, 22-31, 10.1016/j.atmosenv.2012.09.012, 2012.
Vidović, K., Kroflič, A., Šala, M., and Grgić, I.: Aqueous-phase brown carbon formation from aromatic precursors under sunlight conditions, Atmosphere, 11, 131, 2020.
Wang, D., Shen, Z., Zhang, Q., Lei, Y., Zhang, T., Huang, S., Sun, J., Xu, H., and Cao, J.: Winter brown carbon over six of China's megacities: light absorption, molecular characterization, and improved source apportionment revealed by multilayer perceptron neural network, Atmospheric Chemistry and Physics, 22, 14893-14904, 10.5194/acp-22-14893-2022, 2022a.
Wang, Q. Q., Zhou, Y. Y., Ma, N., Zhu, Y., Zhao, X. C., Zhu, S. W., Tao, J. C., Hong, J., Wu, W. J., Cheng, Y. F., and Su, H.: Review of brown carbon aerosols in China: Pollution level, optical properties, and emissions, Journal of Geophysical Research: Atmospheres, 127, 10.1029/2021JD035473, 2022b.
Wang, Y., Pavuluri, C. M., Fu, P., Li, P., Dong, Z., Xu, Z., Ren, H., Fan, Y., Li, L., Zhang, Y.-L., and Liu, C.-Q.: Characterization of Secondary Organic Aerosol Tracers over Tianjin, North China during Summer to Autumn, ACS Earth and Space Chemistry, 3, 2339-2352, 10.1021/acsearthspacechem.9b00170, 2019.
Wen, H., Zhou, Y., Xu, X., Wang, T., Chen, Q., Chen, Q., Li, W., Wang, Z., Huang, Z., Zhou, T., Shi, J., Bi, J., Ji, M., and Wang, X.: Water-soluble brown carbon in atmospheric aerosols along the transport pathway of Asian dust: Optical properties, chemical compositions, and potential sources, Science of the Total Environment, 789, 147971, 10.1016/j.scitotenv.2021.147971, 2021.
Wong, J. P. S., Nenes, A., and Weber, R. J.: Changes in light absorptivity of molecular weight separated brown carbon due to photolytic aging, Environmental Science & Technology, 51, 8414-8421, 10.1021/acs.est.7b01739, 2017.
Wu, G., Fu, P., Ram, K., Song, J., Chen, Q., Kawamura, K., Wan, X., Kang, S., Wang, X., Laskin, A., and Cong, Z.: Fluorescence characteristics of water-soluble organic carbon in atmospheric aerosol, Environmental Pollution, 268, 115906, 10.1016/j.envpol.2020.115906, 2021.
Xie, X., Chen, Y., Nie, D., Liu, Y., Liu, Y., Lei, R., Zhao, X., Li, H., and Ge, X.: Light-absorbing and fluorescent properties of atmospheric brown carbon: A case study in Nanjing, China, Chemosphere, 251, 126350, 10.1016/j.chemosphere.2020.126350, 2020.
Yu, H., Liang, H., Qu, F., Han, Z. S., Shao, S., Chang, H., and Li, G.: Impact of dataset diversity on accuracy and sensitivity of parallel factor analysis model of dissolved organic matter fluorescence excitation-emission matrix, Scientific Reports, 5, 10207, 10.1038/srep10207, 2015.
Yue, S., Zhu, J., Chen, S., Xie, Q., Li, W., Li, L., Ren, H., Sihui, S., Ping, L., Ma, H., Fan, Y., Cheng, B., Wu, L., Deng, J., Hu, W., Ren, L., Lianfang, W., Zhao, W., Tian, Y., and Fu, P.: Brown carbon from biomass burning imposes strong circum-Arctic warming, One Earth, 5, 293-304, 10.1016/j.oneear.2022.02.006, 2022.
Zhang, Q., Jimenez, J. L., Canagaratna, M. R., Ulbrich, I. M., Ng, N. L., Worsnop, D. R., and Sun, Y.: Understanding atmospheric organic aerosols via factor analysis of aerosol mass spectrometry: a review, Analytical Chemistry and Bioanalytical Chemistry, 401, 3045-3067, 10.1007/s00216-011-5355-y, 2011.
Zhao, Z.-Y., Cao, F., Zhang, W.-Q., Zhai, X.-Y., Fang, Y., Fan, M.-Y., and Zhang, Y.-L.: Determination of stable nitrogen and oxygen isotope ratios in atmospheric aerosol nitrates, Chinese Journal of Analytical Chemistry, 47, 907-915, 10.1016/s1872-2040(19)61166-7, 2019.
Zhong, M., and Jang, M.: Light absorption coefficient measurement of SOA using a UV–Visible spectrometer connected with an integrating sphere, Atmospheric Environment, 45, 4263-4271, 10.1016/j.atmosenv.2011.04.082, 2011.
Zhu, C. S., Cao, J. J., Huang, R. J., Shen, Z. X., Wang, Q. Y., and Zhang, N. N.: Light absorption properties of brown carbon over the southeastern Tibetan Plateau, Science of the Total Environment, 625, 246-251, 10.1016/j.scitotenv.2017.12.183, 2018.